Dynamics of heavy quarks in heavy-ion collisions

Elena Bratkovskaya

(GSI, Darmstadt & Uni. Frankfurt)

In collaboration with Taesoo Song, Pierre Moreau, Wolfgang Cassing, Hamza Berrehrah, Olga Soloveva, Laura Tolos, Juan Torres-Rincon, Jörg Aichelin, Pol-Bernard Gossiaux

INT Workshop "Heavy Flavor Production in Heavy-Ion and Elementary Collisions"
3-8 October 2022, INT, Seattle, USA

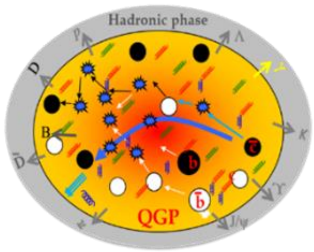

Motivation

The goal: study of the properties of hot and dense nuclear and partonic matter by ‚charm probes‘ (or heavy quark probes)

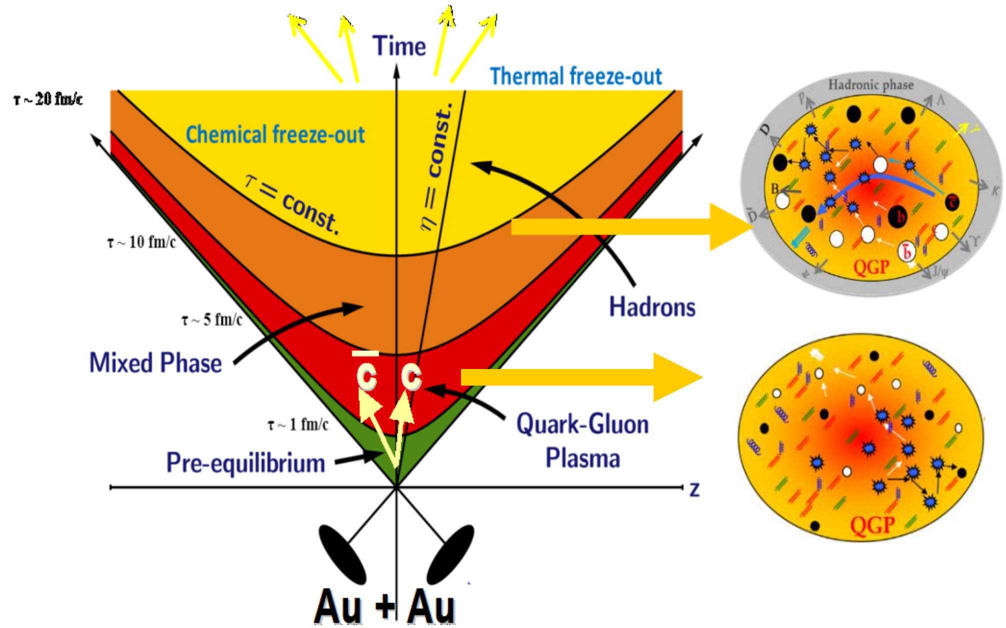

The advantages of the ’charm probes’:

- ❑ dominantly produced in the very early stages of the reactions in initial binary collisions with large energy-momentum transfer

- ❑ initial charm production is well described by pQCD – FONLL

- ❑ heavy quark scattering cross sections are small (compared to the light quarks) ➔ not in an equilibrium with the surrounding matter

- ❑ sensitive to the properties of the QGP during the expansion (and not only to its final state)

➔ **Hope to use ’charm probes’ for an early tomography of the QGP**

Dynamical description of hard probes

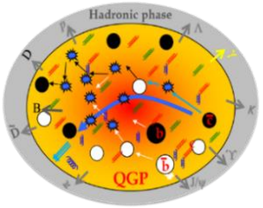

I. Modeling of time evolution of the ‚medium' = system:

- expanding fireball models ← assumption of global equilibrium
- ideal or viscous hydrodynamical models ← assumption of local equilibrium
- microscopic transport models ← full non-equilibrium dynamics!

II. Modeling of the interaction of the hard probes with the ‚medium':

- Fokker-Planck model, Langevin model ← transport coefficients $A = dp_{\mathrm{L}}/dt, \quad \hat{q} = dp_{\mathrm{T}}^2/dt$
- linear Boltzmann models ← cross sections
- microscopic collision integral ← cross sections

	coupling	mass in gluon propagator	mass in external legs
1)	$\alpha(Q^2)$	$\kappa = 0.2, m_D$	$m_{q,g} = 0$
2)	$\alpha(Q^2)$	$\kappa = 0.2, m_D$	$m_{q,g} = m_{q,g}^{DQPM}$
3)	$\alpha(T)$	$\kappa = 0.2, m_D$	$m_{q,g} = 0$
4)	$\alpha(T)$	m_g^{DQPM}	$m_{q,g} = m_{q,g}^{DQPM}$
5)	$\alpha(T)$	m_g^{DQPM}	$m_{q,g} = 0$
6)	$\alpha(Q^2)$	m_g^{DQPM}	$m_{q,g} = m_{q,g}^{DQPM}$

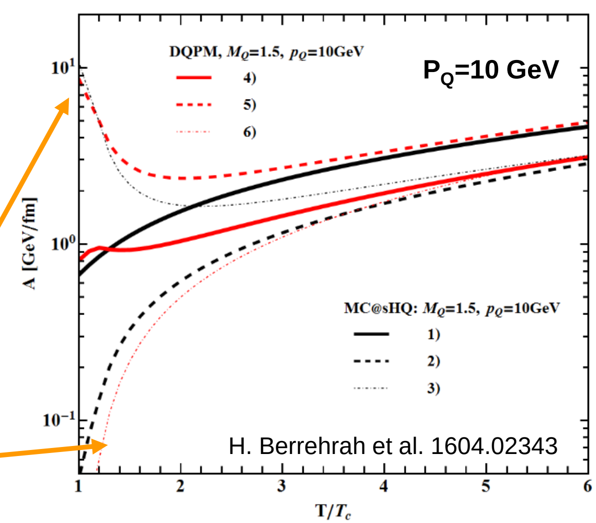

Highlights of model comparisons

EMMI-charm: R. Rapp et al., NPA979 (2018) 21-86; **"Jet"-charm:** S. Cao et al., PRC 99, 054907 (2019)
Frankfurt-Duke-Nantes-Catania: Y. Xu et al., PRC 99 (2019), 014902; T. Song et al., PRC 101 (2020) 044901; ibid. 044903

- ❑ **interaction of heavy quarks with medium; charm transport coefficients; initial conditions; comparison: Langevin vs. Boltzmann description;**
- ❑ **hydro vs. microscopic transport description of the medium; non-equilibrium effects etc.**

Y. Xu et al., PRC 99 (2019), 014902

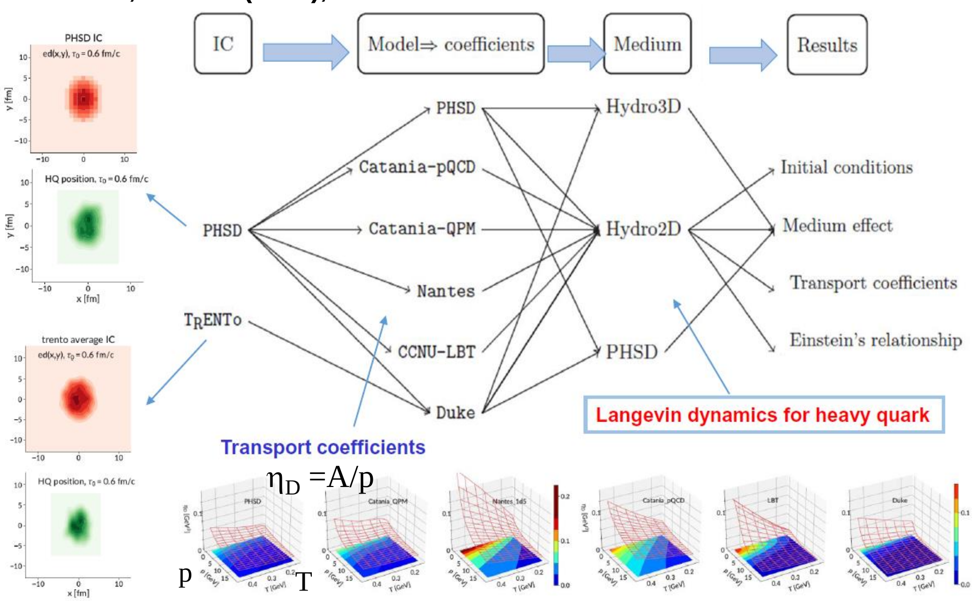

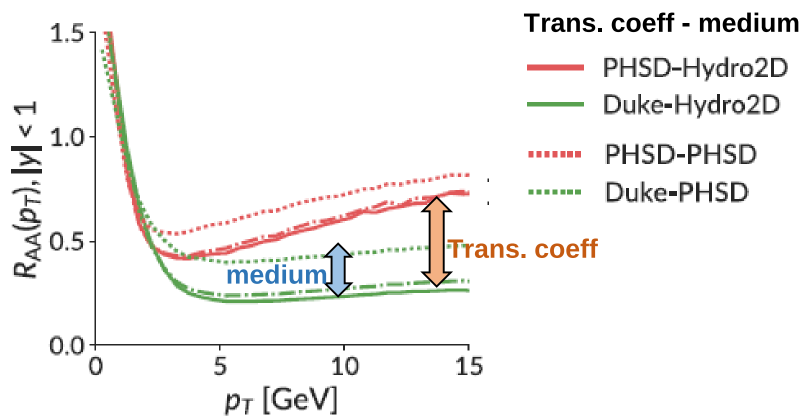

➔ **Charm quarks are sensitive to the history of the QGP evolution and retain information on the entire time evolution from initial condition up to the late stage of the reaction**

- ❑ **Initial conditions: larger effect (up to 20%) on v_2 than on R_{AA}**
- ❑ **Transport coefficients: huge influence on R_{AA} and v_2 within Langevin models**
- ❑ **Medium evolution: R_{AA} and v_2 from nonequilibrium transport differ from hydro and Langevin results**

➔ **Langevin models are not an appropriate tool to study the charm dynamics in HICs!**
➔ **Microscopic transport description of HIC dynamics (medium) and charm interactions (based on Boltzmann collision terms) is required**

Dynamical Models → PHSD

The goal:

to describe the dynamics of charm quarks/mesons in all phases of HICs on a microscopic basis

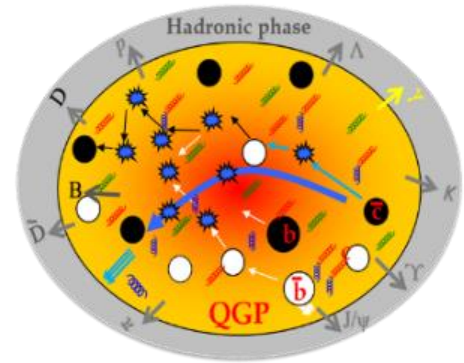

Realization:

a dynamical non-equilibrium transport approach

- **applicable for strongly interacting systems,**
- **which includes a phase transition from hadronic matter to QGP**

The tool: PHSD approach

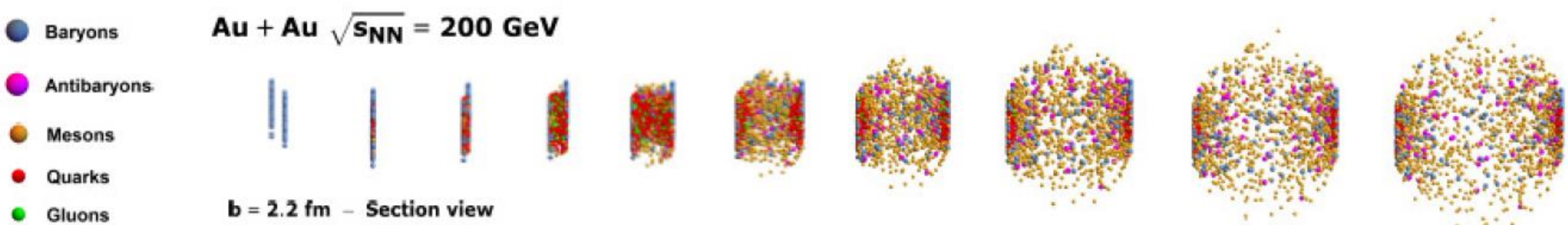

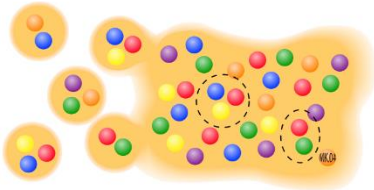

Degrees-of-freedom of QGP

For the microscopic transport description of the system one **needs to know all degrees of freedom** as well as their properties and interactions!

- ❖ **lQCD gives QGP EoS at finite μ_B**

! need to be interpreted in terms of degrees-of-freedom

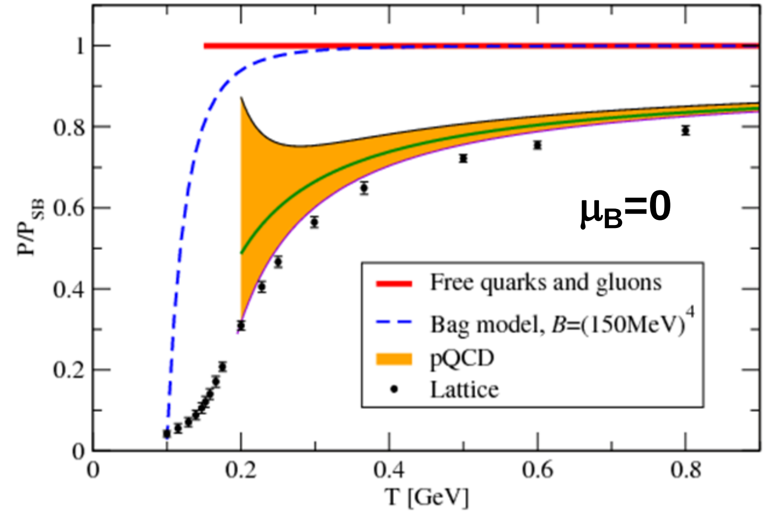

Non-perturbative QCD ← pQCD

pQCD:

- ❑ **weakly interacting system**
- ❑ **massless quarks and gluons**

Thermal QCD
= QCD at high parton densities:

- ❑ **strongly interacting system**
- ❑ **massive quarks and gluons**

➔ quasiparticles
= effective degrees-of-freedom

How to learn about the degrees-of-freedom of the QGP from HICs?
➔ microscopic transport approaches
➔ comparison to HIC experiments

Thermal QCD →

DQPM (T, μ_q)

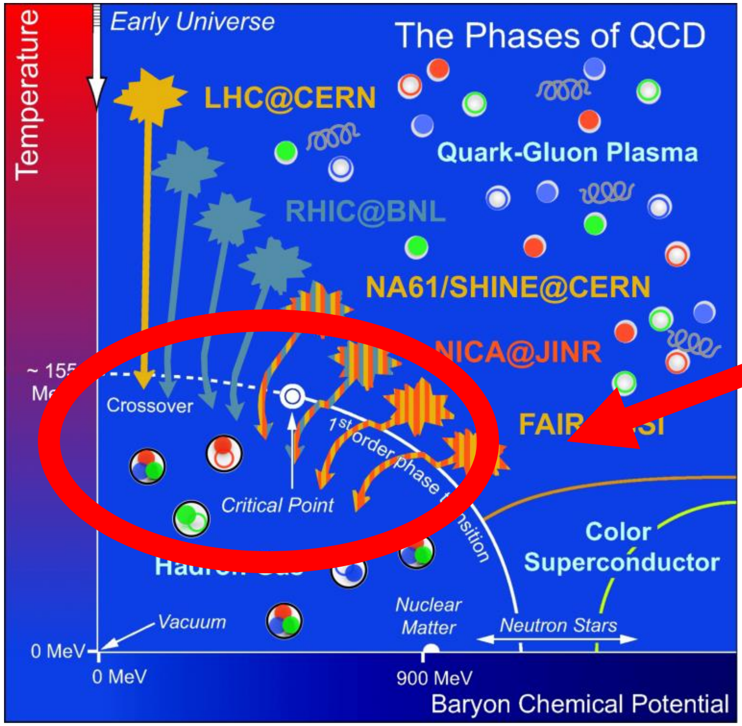

finite T,μ_q

Dynamical QuasiParticle Model (DQPM)

DQPM – effective model for the description of non-perturbative (strongly interacting) QCD based on lQCD EoS

Degrees-of-freedom: strongly interacting dynamical quasiparticles - quarks and gluons

Theoretical basis :

- **‚resummed‘ single-particle Green‘s functions → quark (gluon) propagator (2PI) :**

gluon propagator: $\Delta^{-1} = P^2 - \Pi$ &	quark propagator $S_q^{-1} = P^2 - \Sigma_q$
gluon self-energy: $\Pi = M_g^2 - i2\gamma_g\omega$ &	quark self-energy: $\Sigma_q = M_q^2 - i2\gamma_q\omega$

Properties of the quasiparticles are specified by scalar complex self-energies:

$Re\Sigma_q$: thermal masses (M_g, M_q); $Im\Sigma_q$: interaction widths (γ_g, γ_q)

→ spectral functions $\rho_q = -2ImS_q$ → Lorentzian form:

$$\rho_j(\omega, \mathbf{p}) = \frac{\gamma_j}{\tilde{E}_j}\left(\frac{1}{(\omega - \tilde{E}_j)^2 + \gamma_j^2} - \frac{1}{(\omega + \tilde{E}_j)^2 + \gamma_j^2}\right)$$

$$\equiv \frac{4\omega\gamma_j}{\left(\omega^2 - \mathbf{p}^2 - M_j^2\right)^2 + 4\gamma_j^2\omega^2} \qquad \tilde{E}_j^2(\mathbf{p}) = \mathbf{p}^2 + M_j^2 - \gamma_j^2$$

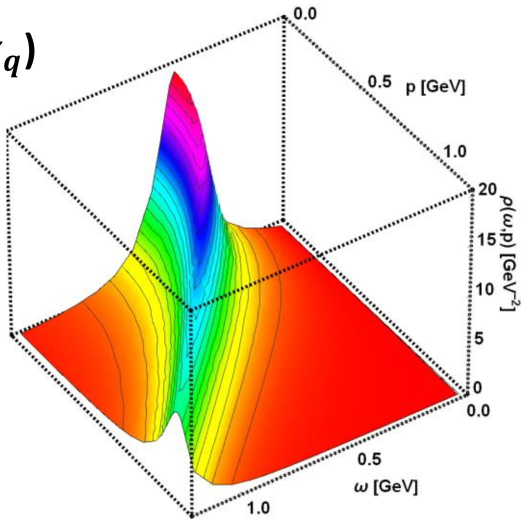

A. Peshier, W. Cassing, PRL 94 (2005) 172301; W. Cassing, NPA 791 (2007) 365: NPA 793 (2007), H. Berrehrah et al, Int.J.Mod.Phys. E25 (2016) 1642003; P. Moreau et al., PRC100 (2019) 014911; O. Soloveva et al., PRC101 (2020) 045203

Parton properties

- Modeling of the quark/gluon masses and widths (ansatz inspired by HTL calculations)

Masses:

$$M^2_{q(\bar{q})}(T,\mu_B) = \frac{N_c^2-1}{8N_c} g^2(T,\mu_B) \left(T^2 + \frac{\mu_q^2}{\pi^2} \right)$$

$$M^2_g(T,\mu_B) = \frac{g^2(T,\mu_B)}{6} \left(\left(N_c + \frac{1}{2} N_f \right) T^2 + \frac{N_c}{2} \sum_q \frac{\mu_q^2}{\pi^2} \right)$$

Widths:

$$\gamma_{q(\bar{q})}(T,\mu_B) = \frac{1}{3} \frac{N_c^2-1}{2N_c} \frac{g^2(T,\mu_B)T}{8\pi} \ln \left(\frac{2c}{g^2(T,\mu_B)} + 1 \right)$$

$$\gamma_g(T,\mu_B) = \frac{1}{3} N_c \frac{g^2(T,\mu_B)T}{8\pi} \ln \left(\frac{2c}{g^2(T,\mu_B)} + 1 \right)$$

→ **DQPM :**
only one parameter (c = 14.4) + (T, μ_B)- dependent coupling constant has to be determined from lattice results

- Coupling g: input - lQCD entropy density s function of T at μ_B=0

$$g^2(s/s_{SB}) = d\left((s/s_{SB})^e - 1\right)^f$$

$$s_{SB}^{QCD} = 19/9\pi^2 T^3$$

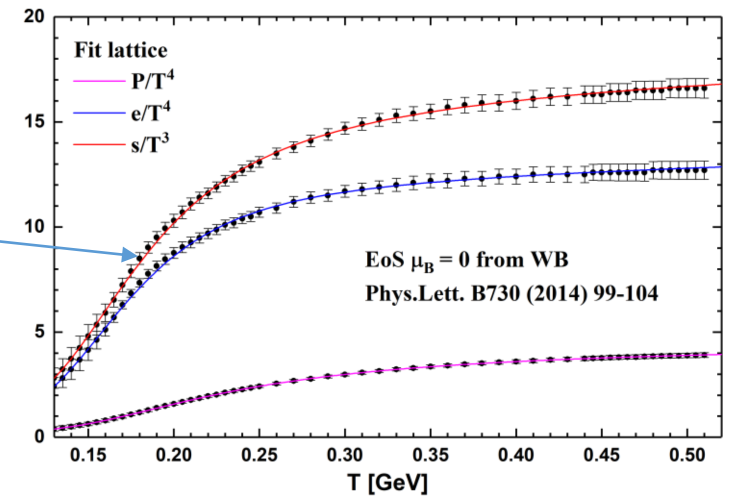

H. Berrehrah et al, PRC 93 (2016) 044914, Int.J.Mod.Phys. E25 (2016) 1642003,

DQPM at finite (T, μ_q): scaling hypothesis

- **Scaling hypothesis for the effective temperature T***
  for $N_f = N_c = 3$ — W. Casssing, NPA 791 (2007) 365

$$\mu_u = \mu_d = \mu_s = \mu_q$$

$$\boxed{T^{*2} = T^2 + \frac{\mu_q^2}{\pi^2}}$$

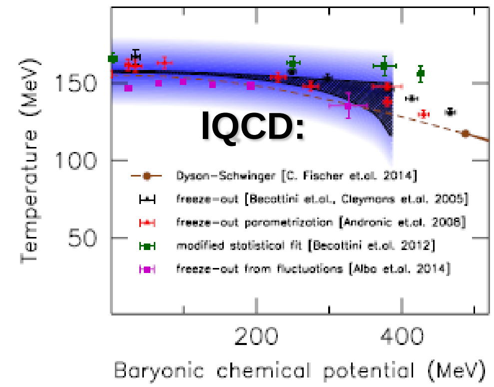

- **Coupling:**

$$g(T/T_c(\mu=0)) \longrightarrow g(T^\star/T_c(\mu))$$

- **Critical temperature $T_c(\mu_q)$ in crossover region:**
  obtained by assuming a constant energy density ε along a critical line $T=T_c(\mu_q)$, where ε at $T_c(\mu_q=0)$=156 GeV is fixed by lQCD at μ_q=0

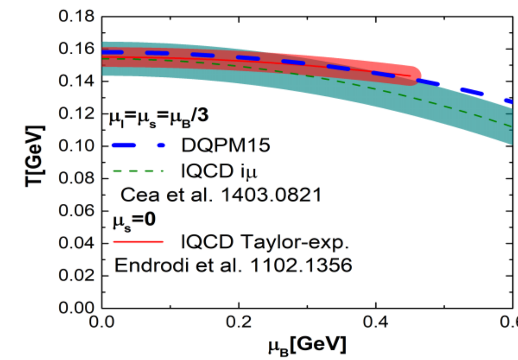

$$\boxed{\frac{T_c(\mu_q)}{T_c(\mu_q=0)} = \sqrt{1-\alpha\,\mu_q^2} \approx 1-\alpha/2\,\mu_q^2+\cdots}$$

$$\alpha \approx 8.79\ \mathrm{GeV}^{-2}$$

! Consistent with lattice QCD:

lQCD: C. Bonati et al., PRC90 (2014) 114025

$$\frac{T_c(\mu_B)}{T_c} = 1-\kappa\left(\frac{\mu_B}{T_c}\right)^2+\cdots$$

lQCD $\kappa = 0.013(2)$ ⟷ $\kappa_{DQPM} \approx 0.0122$

H. Berrehrah et al, PRC 93 (2016) 044914, Int.J.Mod.Phys. E25 (2016) 1642003,

DQPM thermodynamics at finite (T, μ_q)

- **Entropy and baryon density** in the quasiparticle limit (G. Baym 1998):

$$
\begin{aligned}
s^{dqp} = \\
-\int \frac{d\omega}{2\pi}\frac{d^3p}{(2\pi)^3}\Bigg[& d_g \frac{\partial n_B}{\partial T}\left(\mathrm{Im}(\ln \underline{-\Delta^{-1}}) + \mathrm{Im}\,\underline{\Pi}\,\mathrm{Re}\,\underline{\Delta}\right) \\
+ \sum_{q=u,d,s} & d_q \frac{\partial n_F(\omega-\mu_q)}{\partial T}\left(\mathrm{Im}(\ln -\underline{S_q^{-1}}) + \mathrm{Im}\,\underline{\Sigma_q}\,\mathrm{Re}\,\underline{S_q}\right) \\
+ \sum_{\bar q=\bar u,\bar d,\bar s} & d_{\bar q} \frac{\partial n_F(\omega+\mu_q)}{\partial T}\left(\mathrm{Im}(\ln -\underline{S_{\bar q}^{-1}}) + \mathrm{Im}\,\underline{\Sigma_{\bar q}}\,\mathrm{Re}\,\underline{S_{\bar q}}\right)\Bigg]
\end{aligned}
$$

$$
\begin{aligned}
n^{dqp} = -\int \frac{d\omega}{2\pi}\frac{d^3p}{(2\pi)^3} \\
\Bigg[\sum_{q=u,d,s} & d_q \frac{\partial n_F(\omega-\mu_q)}{\partial \mu_q}\left(\mathrm{Im}(\ln -\underline{S_q^{-1}}) + \mathrm{Im}\,\underline{\Sigma_q}\,\mathrm{Re}\,\underline{S_q}\right) \\
+ \sum_{\bar q=\bar u,\bar d,\bar s} & d_{\bar q} \frac{\partial n_F(\omega+\mu_q)}{\partial \mu_q}\left(\mathrm{Im}(\ln -\underline{S_{\bar q}^{-1}}) + \mathrm{Im}\,\underline{\Sigma_{\bar q}}\,\mathrm{Re}\,\underline{S_{\bar q}}\right)\Bigg]
\end{aligned}
$$

B. Vanderheyden, G. Baym, J. Stat. Phys. 93 (1998) 843
Blaizot, Iancu, Rebhan, Phys. Rev. D 63 (2001) 065003

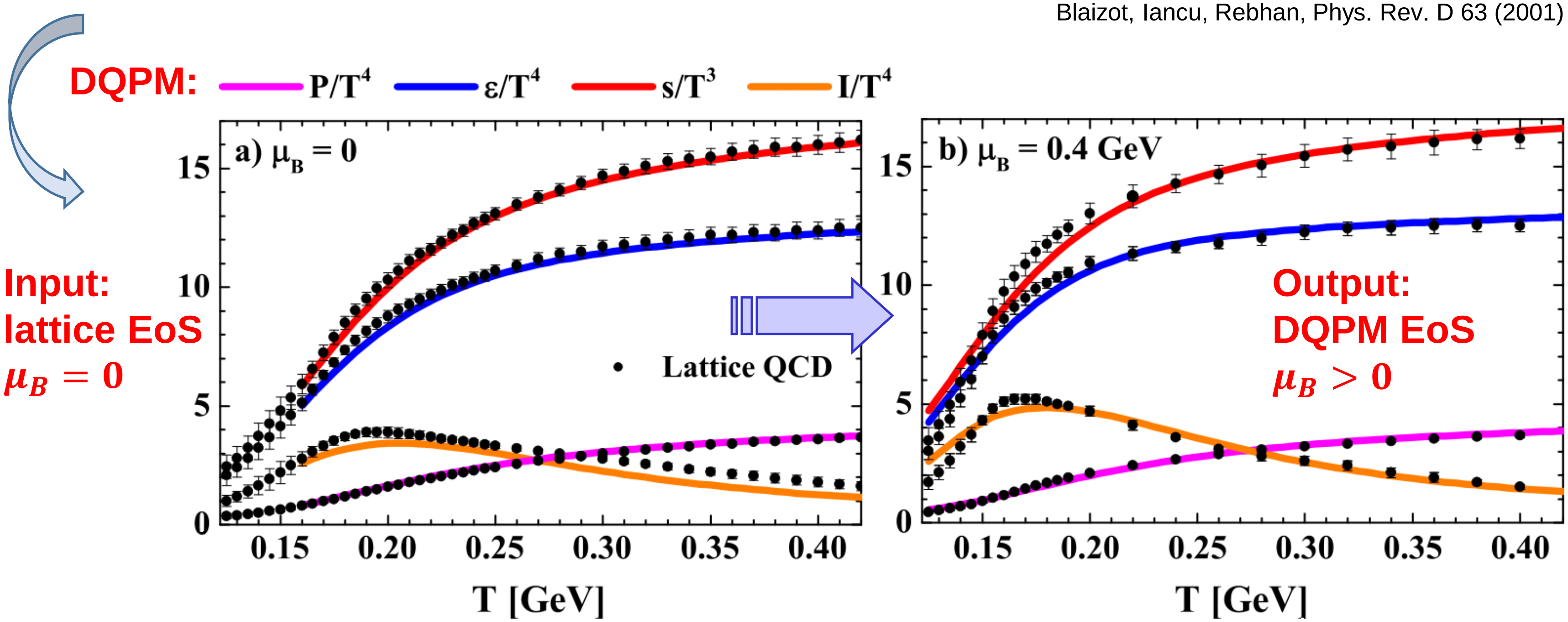

lQCD: Sz. Borsanyi et al., JHEP 1208 (2012) 053

DQPM: parton properties

Coupling as a function of (T, μ_B)

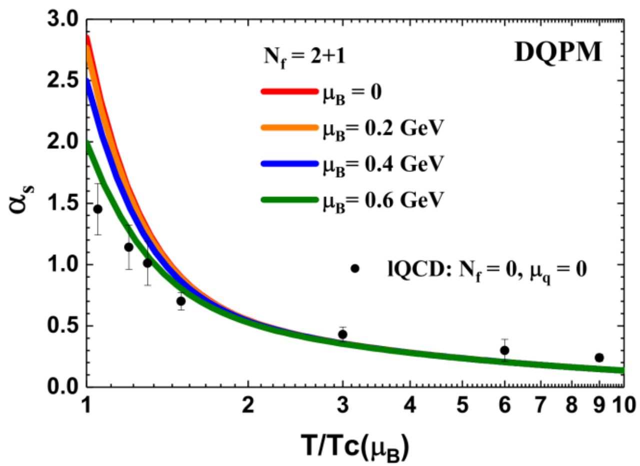

➔ Lorentzian spectral function:

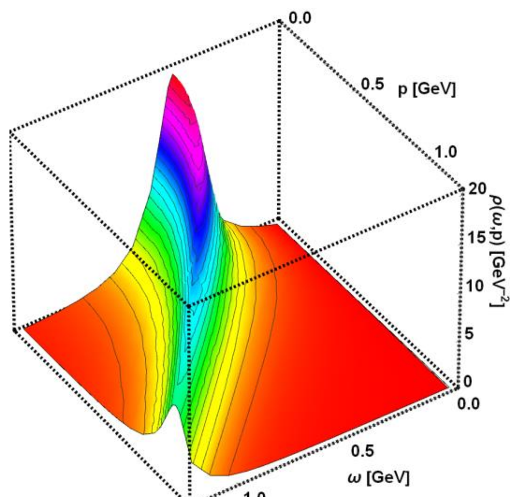

Pole masses and widths vs (T, μ_B)

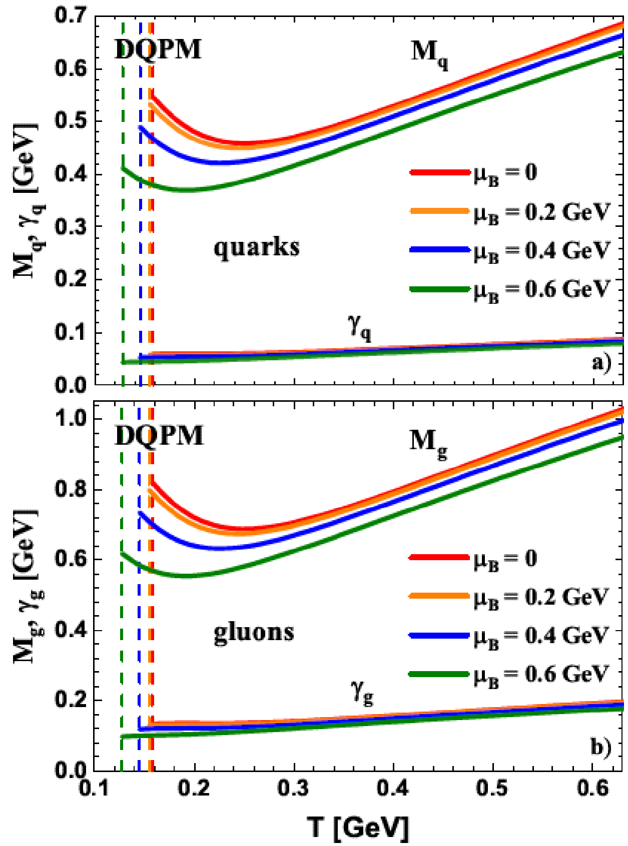

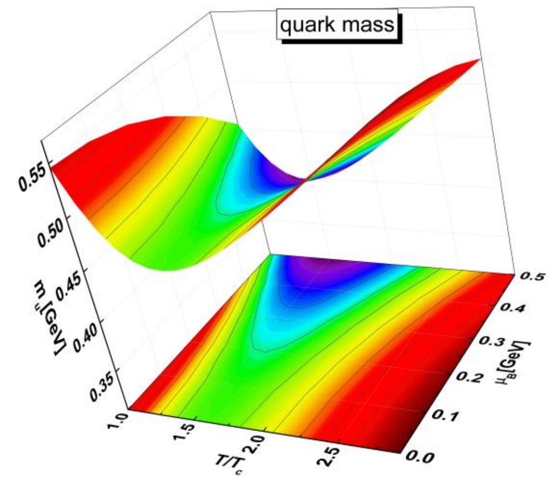

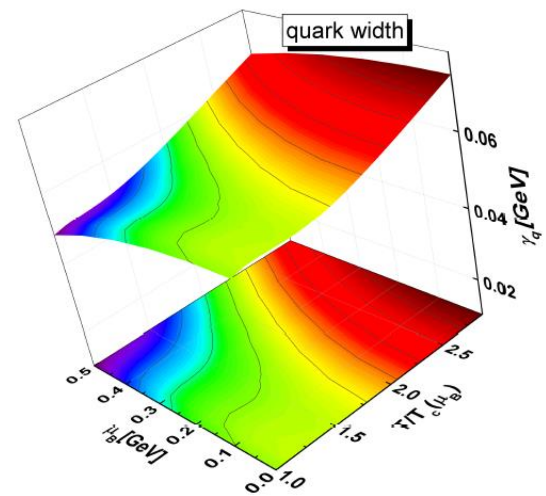

P. Moreau et al., PRC100 (2019) 014911

Partonic interactions: matrix elements

DQPM partonic cross sections → leading order diagrams

- **Propagators for massive bosons and fermions:**

$$= -i\delta_{ab}\frac{g^{\mu\nu} - q^\mu q^\nu / M_g^2}{q^2 - M_g^2 + 2i\gamma_g q_0}$$

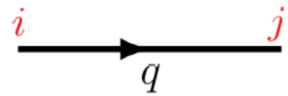

$$= i\delta_{ij}\frac{\not{q} + M_q}{q^2 - M_q^2 + 2i\gamma_q q_0}$$

- **(Quasi-) elastic channels:**

qq' → qq' scattering

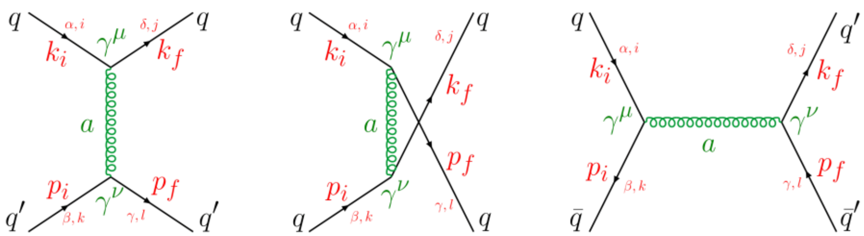

t − channel u − channel s − channel

gq → gq scattering

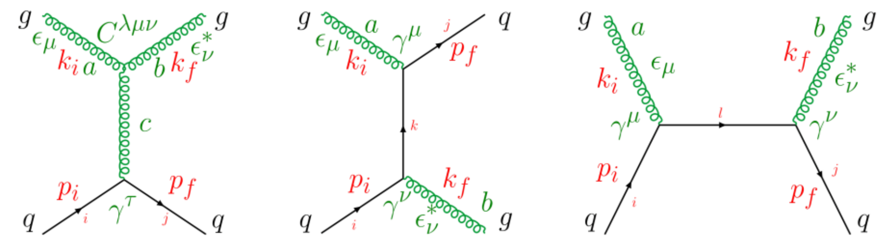

t − channel u − channel s − channel

gg→ gg scattering

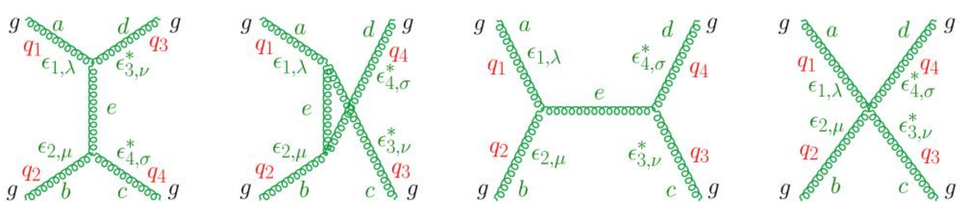

t − channel u − channel s − channel 4 − point

- **Inelastic channels:**

$$\mathrm{q} + \bar{\mathrm{q}} \rightarrow \mathrm{g}$$
$$\mathrm{g} \rightarrow \mathrm{q} + \bar{\mathrm{q}}$$

H. Berrehrah et al, PRC 93 (2016) 044914, Int.J.Mod.Phys. E25 (2016) 1642003, → **P. Moreau et al., PRC100 (2019) 014911**

Differential cross sections

- **On-shell:**

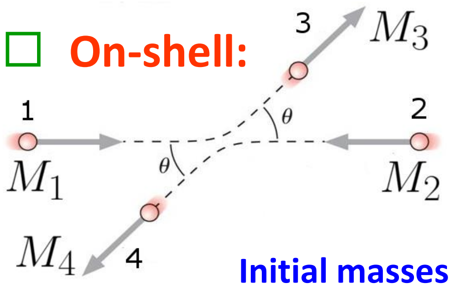

Initial masses: pole masses
Final masses: pole masses

- **Off-shell:**

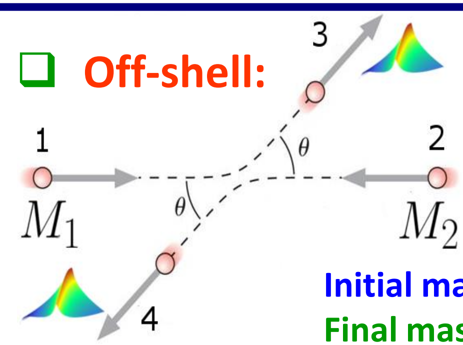

Initial masses: pole masses
Final masses: integration over spectral functions

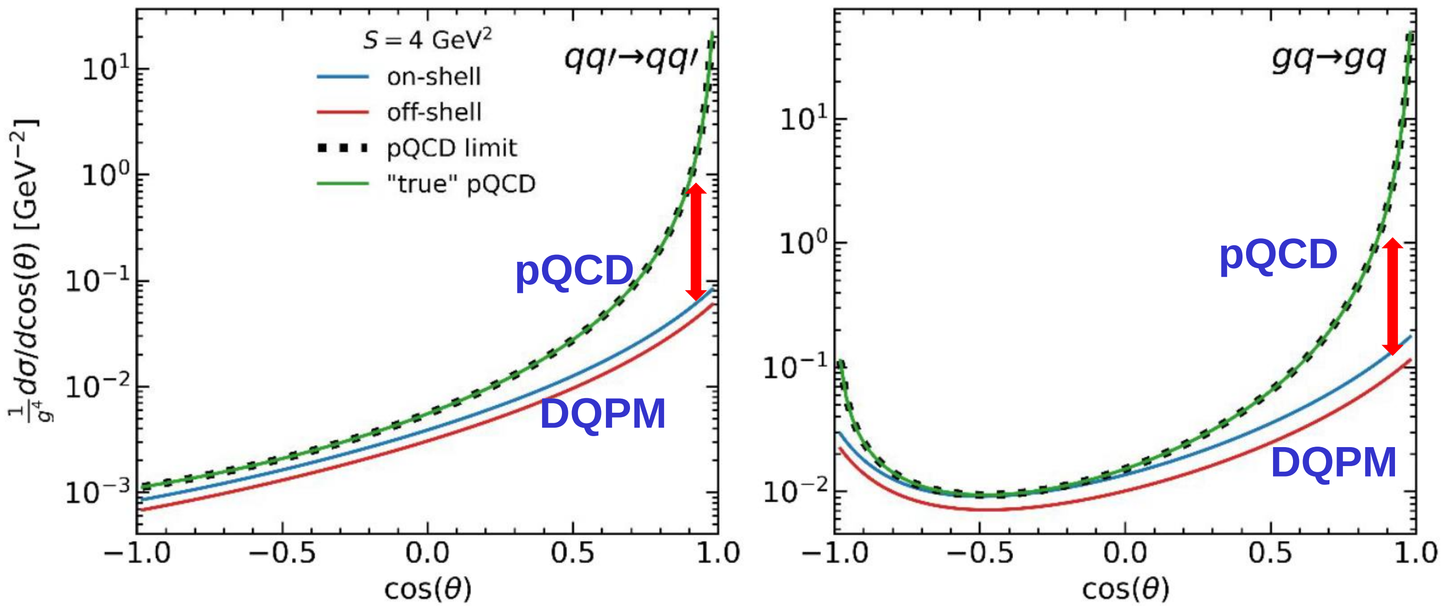

- **DQPM: M→0, γ→0 ➔ reproduces pQCD limits**
- **Differences between DQPM and pQCD : less forward peaked angular distribution leads to more efficient momentum transfer**

P. Moreau et al., PRC100 (2019) 014911

Total cross section

□ **On-shell:**

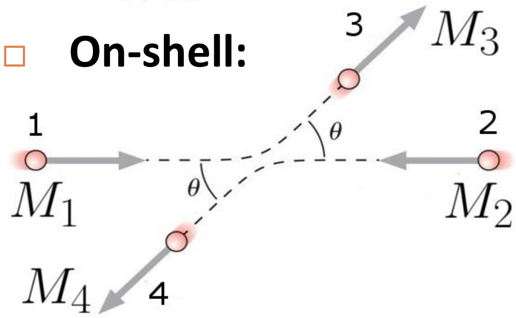

□ **Off-shell:**

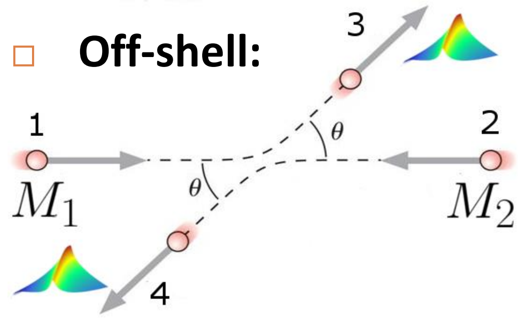

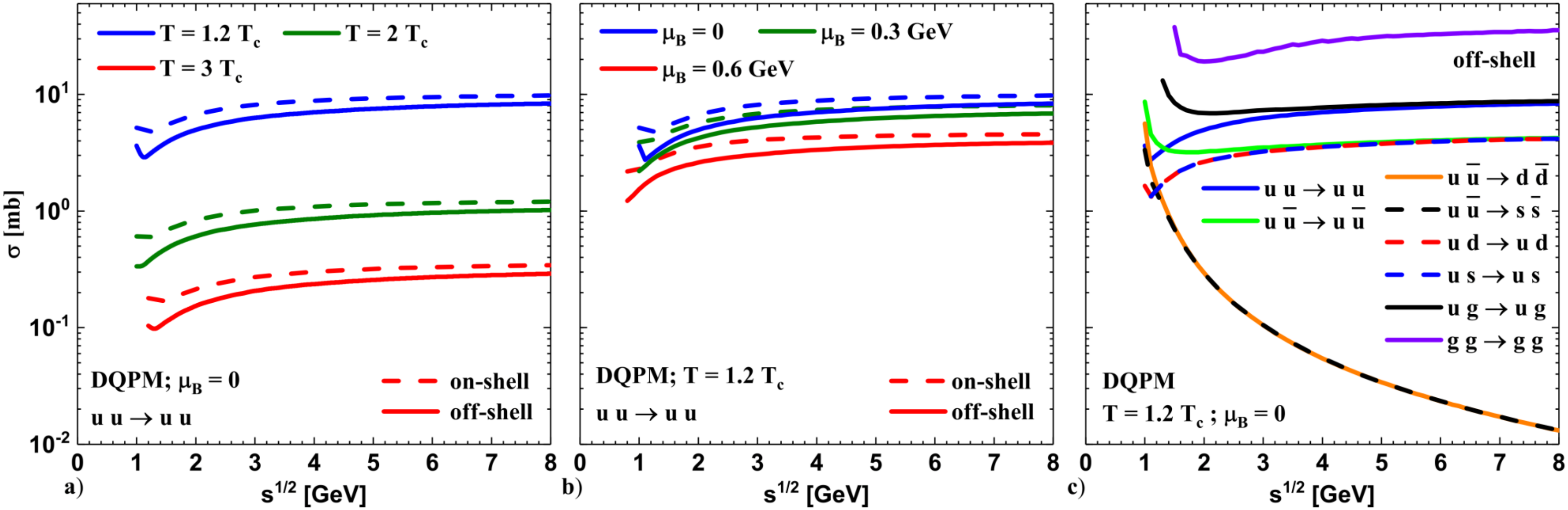

- ❑ **strong *T* dependence**
- ❑ **weak μ_B dependence**
- ❑ **strong channel dependence**

P. Moreau et al., PRC100 (2019) 014911

Transport coefficients: shear viscosity η

➢ Relaxation Time Approximation

$$\eta^{\mathrm{RTA}}(T,\mu_B) = \frac{1}{15T}\sum_{i=q,\bar{q},g}\int \frac{d^3p}{(2\pi)^3}\frac{\mathbf{p}^4}{E_i^2}\boxed{\tau_i(\mathbf{p},T,\mu_B)}\, d_i(1\pm f_i)f_i$$

Relaxation time:

$$1)\,\tau_i(\mathbf{p},T,\mu_B) = \frac{1}{\Gamma_i(\mathbf{p},T,\mu_B)}$$

$$2)\,\tau_i(T,\mu_B) = \frac{1}{2\gamma_i(T,\mu_B)},$$

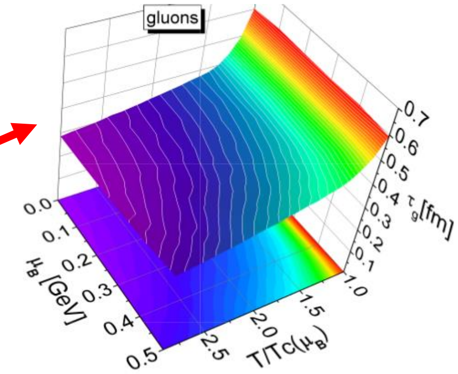

Interaction rate:

$$\Gamma_i^{\mathrm{on}}(\mathbf{p}_i,T,\mu_q) = \frac{1}{2E_i}\sum_{j=q,\bar{q},g}\int\frac{d^3p_j}{(2\pi)^3 2E_j}\, d_j\ f_j(E_j,T,\mu_q)$$
$$\int\frac{d^3p_3}{(2\pi)^3 2E_3}\int\frac{d^3p_4}{(2\pi)^3 2E_4}(1\pm f_3)(1\pm f_4)$$
$$|\bar{\mathcal{M}}|^2(p_i,p_j,p_3,p_4)\ (2\pi)^4\delta^{(4)}\left(p_i+p_j-p_3-p_4\right)$$

η/s versus (T,μ_B)

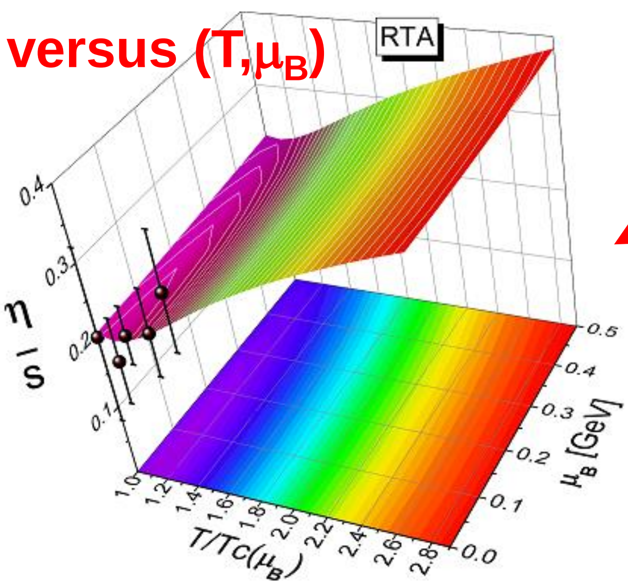

μ_B

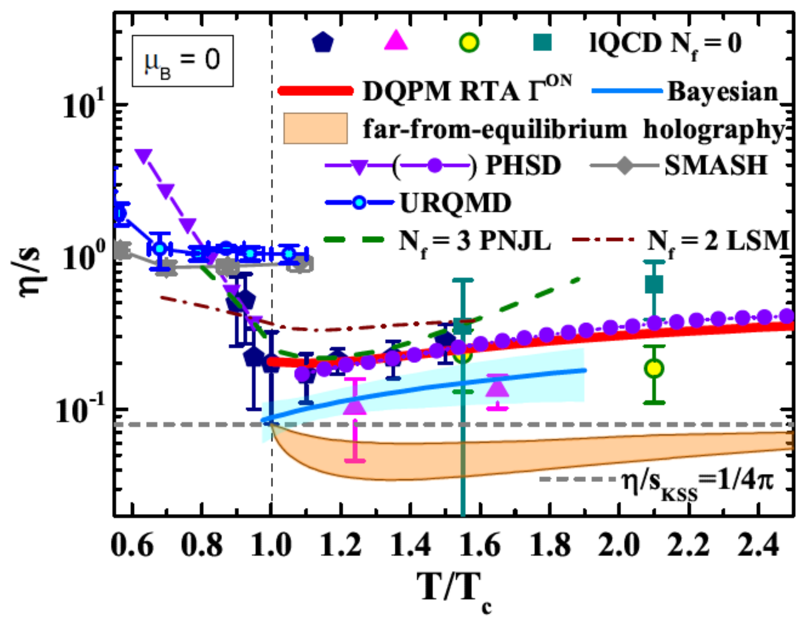

➢ **Good agreement with lQCD**

➢ **Light increase of shear viscosity with μ_B**

Lattice QCD: N. Astrakhantsev et al, JHEP 1704 (2017) 101

P. Moreau et al., PRC100 (2019) 014911; O. Soloveva et al., PRC110 (2020) 045203

Transport coefficients

Bulk viscosity ζ/s

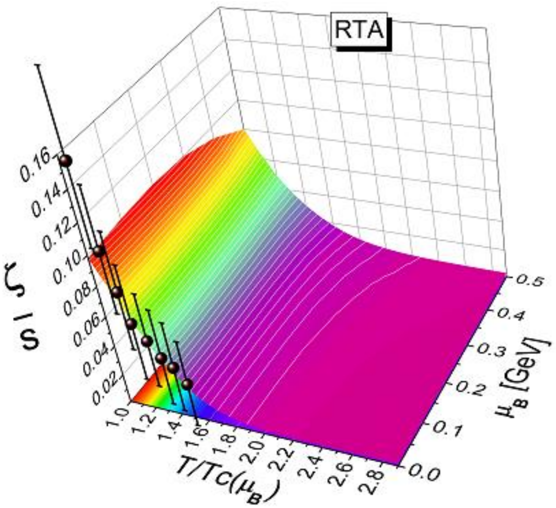

Speed of sound c_s^2

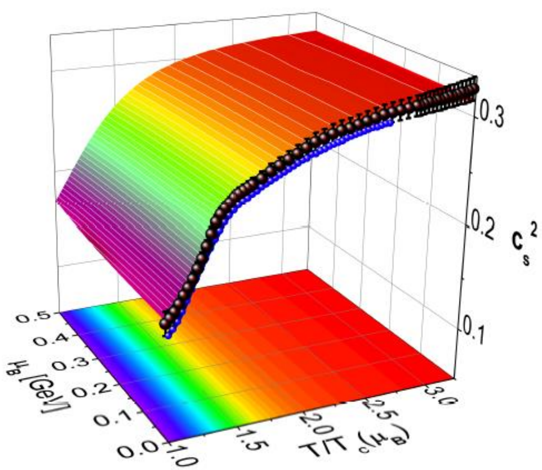

- $\kappa_{qq'}$ (q; q' = B; S; Q) - **diffusion coefficient matrix** for the baryon (B), strange (S) and electric (Q) charges using **Chapman-Enskog method (CE) & RTA**

$$\begin{pmatrix} \kappa_{BB} & \kappa_{BQ} & \kappa_{BS} \\ \kappa_{QB} & \kappa_{QQ} & \kappa_{QS} \\ \kappa_{SB} & \kappa_{SQ} & \kappa_{SS} \end{pmatrix}$$

Electric conductivity σ_e/T

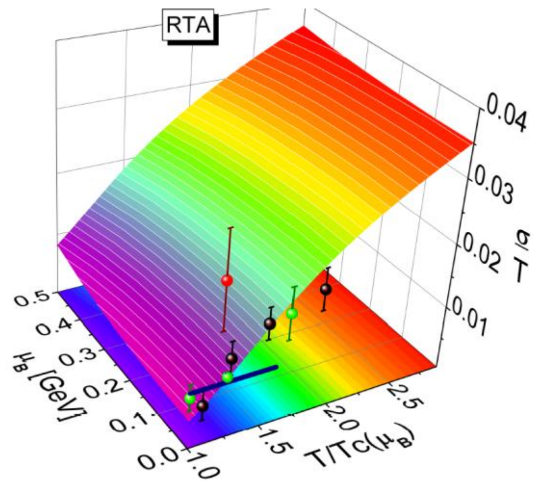

Baryon diffusion coefficient κ_B/T^2

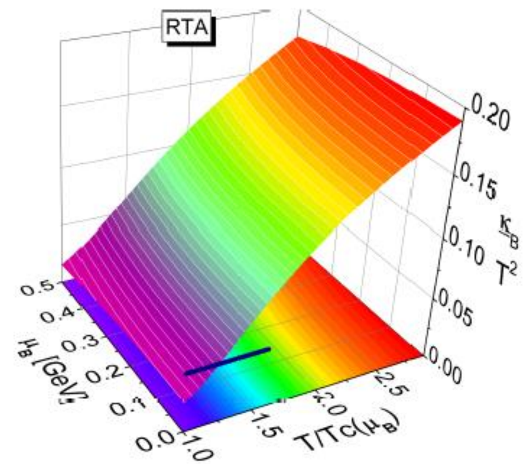

J. A. Fotakis, O. S., C. Greiner, O. Kaczmarek and E. Bratkovskaya PRD 104 (2021) , 034014

P. Moreau et al., PRC100 (2019) 014911; O. Soloveva et al., PRC110 (2020) 045203

Transport coefficients: $\hat{q}$

The jet transport coefficient $\hat{q}$
in non-perturbative strongly interacting QGP
(DQPM):

$$\boxed{\hat{q}(p) = \frac{d\langle(\Delta p_T)^2\rangle}{dx}}$$

Elastic scattering of jet
parton with off-shell
partons from sQGP:

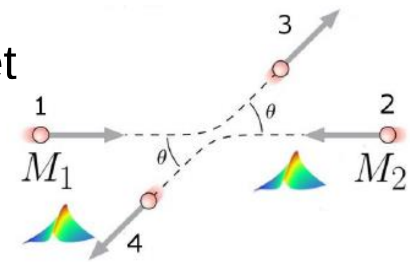

$$\langle\langle O^* \rangle\rangle \equiv \frac{1}{2E_p} \sum_{i=q,\bar{q},g} \int dm \rho_i(m) \int dm' \rho_i(m')$$
$$\times \int \frac{d^3k}{(2\pi)^3 2E} f_i(k, m_i) \int \frac{d^3k'}{(2\pi)^3 2E'} \int \frac{d^3p'}{(2\pi)^3 2E'_p}$$
$$\times O^* \, (2\pi)^4 \delta^{(4)}(p + q - p' - q') \frac{|M_{ic}|^2}{\gamma_c},$$

$\rho_i(m)$ – parton spectral function

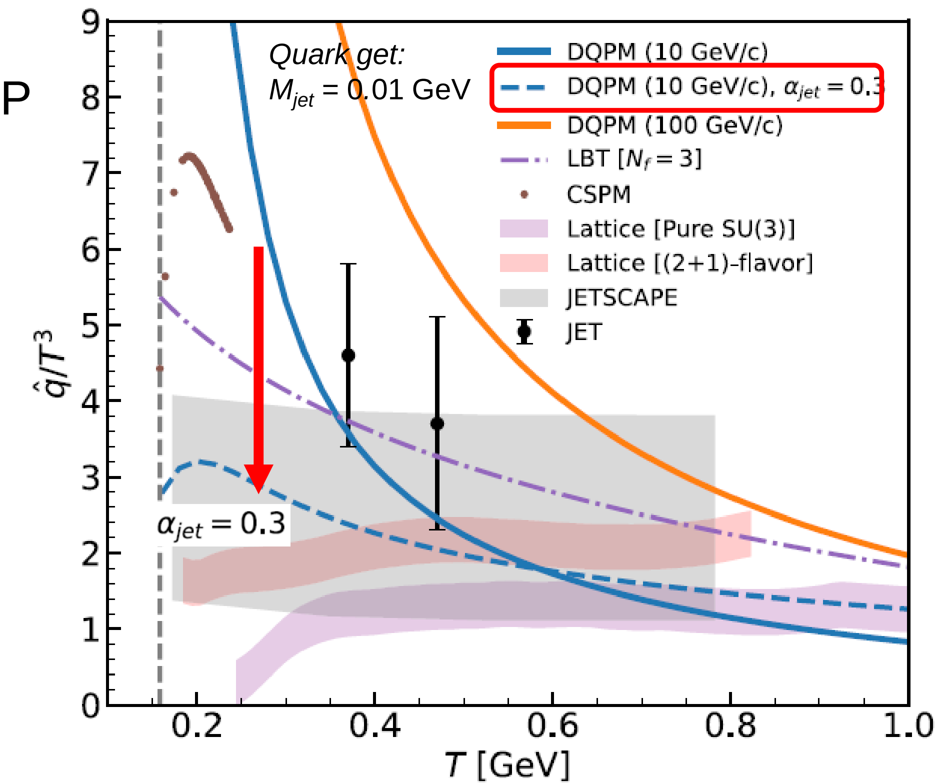

Quark jet :

$$\langle \mathcal{O} \rangle = \langle \mathcal{O} \rangle_{uu\to uu} + \langle \mathcal{O} \rangle_{u\bar{u}\to u\bar{u}} + 2\langle \mathcal{O} \rangle_{ud\to ud} + 2\langle \mathcal{O} \rangle_{us\to us} + \langle \mathcal{O} \rangle_{ug\to ug}.$$

Gluon jet :

$$\langle \mathcal{O} \rangle = 4\langle \mathcal{O} \rangle_{gu\to gu} + 2\langle \mathcal{O} \rangle_{gs\to gs} + \langle \mathcal{O} \rangle_{gg\to gg}.$$

Ilia Grishmanovskii et al., Phys. Rev. C 106, 014903 (2022)

QGP:
in-equilibrium → off-equilibrium

Microscopic transport theory!

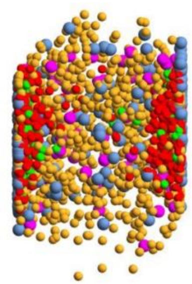

W. Cassing, ‚Transport Theories for Strongly-Interacting Systems', Springer Nature: Lecture Notes in Physics 989, 2021

Parton-Hadron-String-Dynamics (PHSD)

PHSD is a non-equilibrium microscopic transport approach for the description of strongly-interacting hadronic and partonic matter created in heavy-ion collisions

Dynamics: based on the solution of generalized off-shell transport equations derived from Kadanoff-Baym many-body theory

Initial A+A collision

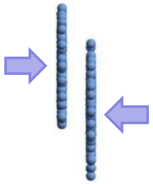

Partonic phase

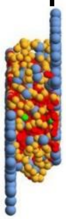

Hadronization

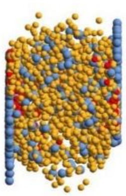

Hadronic phase

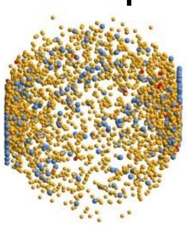

- **Initial A+A collisions :**
  N+N → string formation → decay to pre-hadrons + leading hadrons

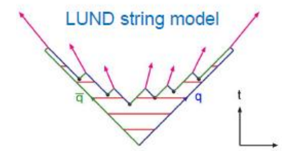

- **Formation of QGP stage if local $\varepsilon > \varepsilon_{critical}$:**
  dissolution of pre-hadrons → partons

- **Partonic phase - QGP:**
  QGP is described by the Dynamical QuasiParticle Model (DQPM) matched to reproduce lattice QCD EoS for finite T and μ_B (crossover)

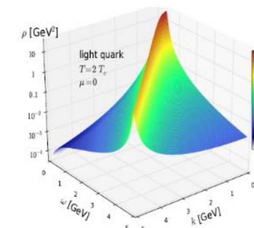

  - **Degrees-of-freedom:** strongly interacting quasiparticles: massive quarks and gluons (g,q,q_{bar}) with sizeable collisional widths in a self-generated mean-field potential
  - **Interactions:** (quasi-)elastic and inelastic collisions of partons

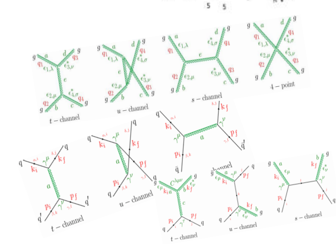

- **Hadronization to colorless off-shell mesons and baryons:**
  Strict 4-momentum and quantum number conservation

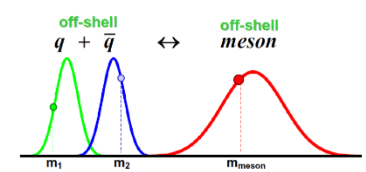

- **Hadronic phase: hadron-hadron interactions – off-shell HSD**

W. Cassing, E. Bratkovskaya, PRC 78 (2008) 034919; NPA831 (2009) 215; W. Cassing, EPJ ST 168 (2009) 3

Stages of a collision in PHSD

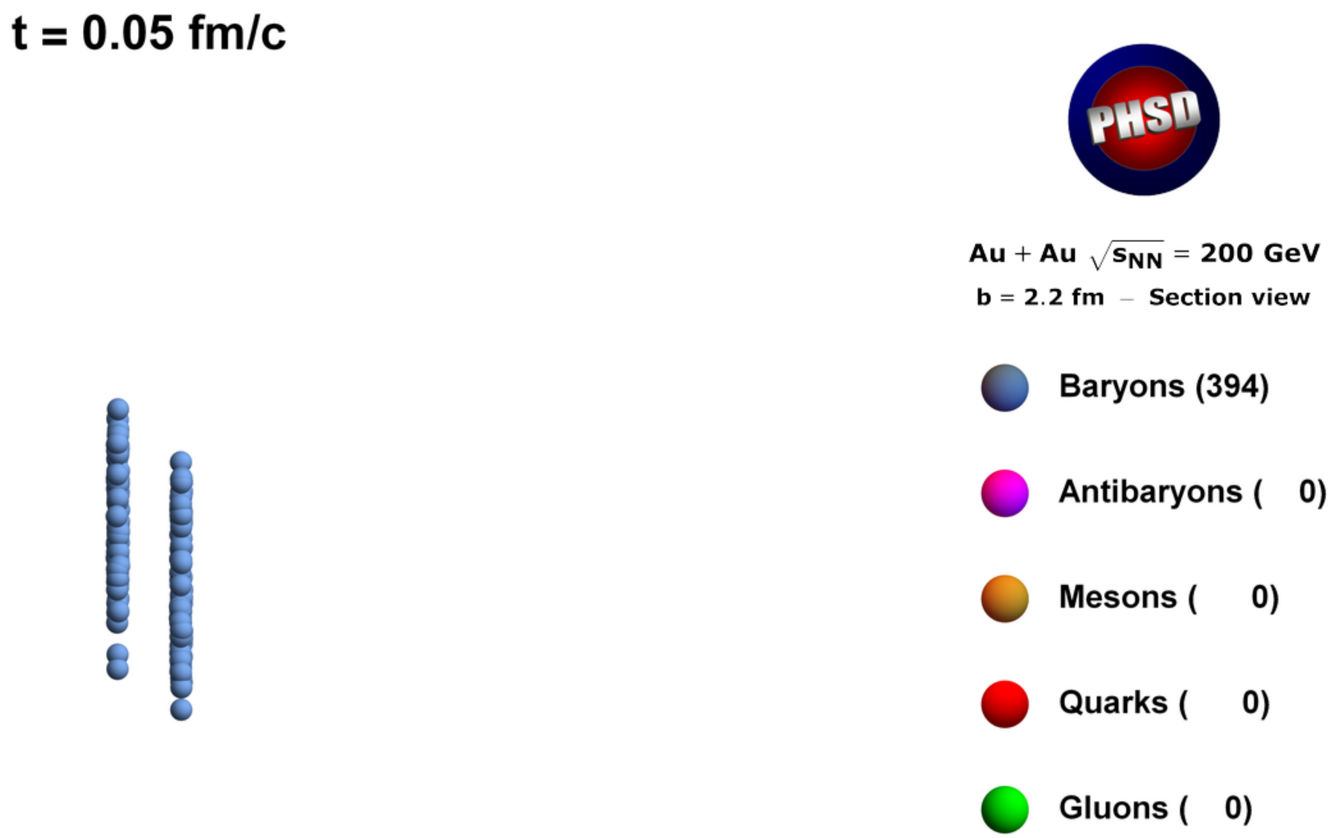

P.Moreau

Stages of a collision in PHSD

t = 1.6512 fm/c

Au + Au $\sqrt{s_{NN}}$ = 200 GeV

b = 2.2 fm – Section view

Baryons (394)

Antibaryons (0)

Mesons (1523)

Quarks (4553)

Gluons (368)

P.Moreau

Stages of a collision in PHSD

t = 3.91921 fm/c

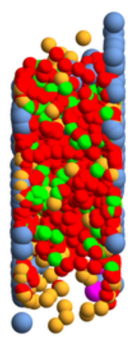

Au + Au $\sqrt{s_{NN}}$ = 200 GeV
b = 2.2 fm – Section view

Baryons (426)
Antibaryons (29)
Mesons (1189)
Quarks (4459)
Gluons (783)

P.Moreau

Stages of a collision in PHSD

t = 7.31921 fm/c

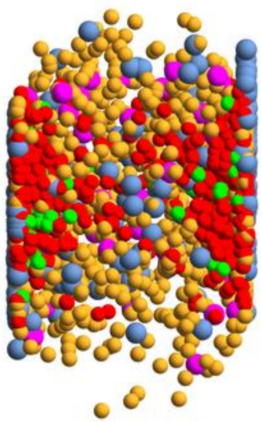

Au + Au $\sqrt{s_{NN}}$ = 200 GeV

b = 2.2 fm – Section view

Baryons (540)

Antibaryons (120)

Mesons (2481)

Quarks (2901)

Gluons (492)

P.Moreau

Stages of a collision in PHSD

t = 12.0192 fm/c

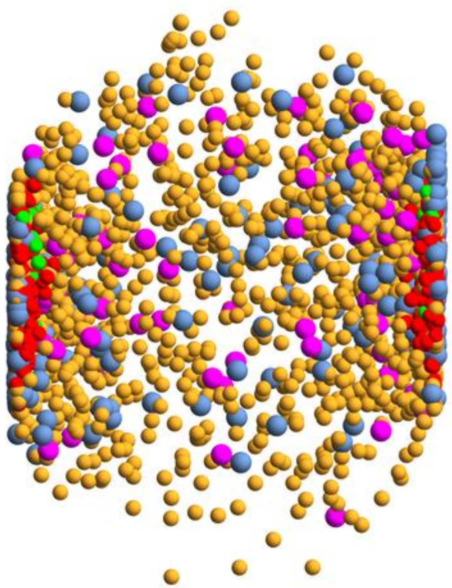

Au + Au $\sqrt{s_{NN}}$ = 200 GeV

b = 2.2 fm – Section view

Baryons (626)

Antibaryons (202)

Mesons (3357)

Quarks (1835)

Gluons (269)

P.Moreau

Stages of a collision in PHSD

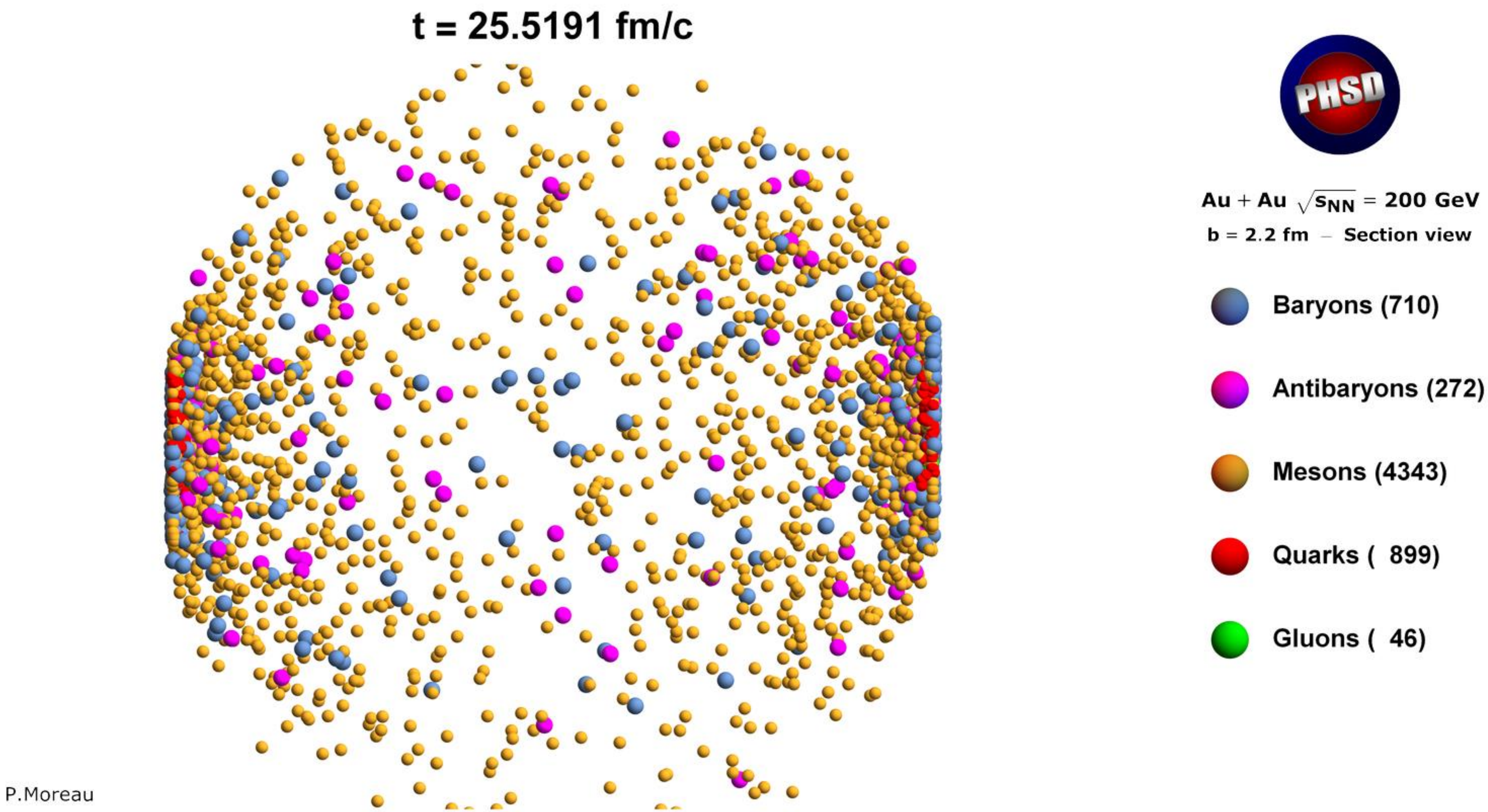

Non-equilibrium dynamics: description of A+A with PHSD

❑ **Important:** to be conclusive on charm observables, the **light quark dynamics** must be well under control!

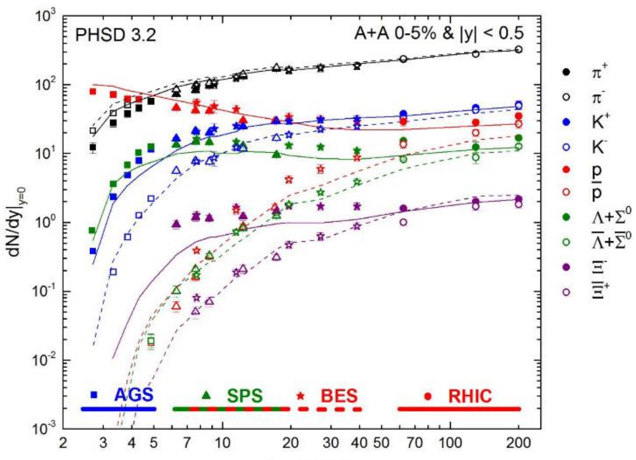

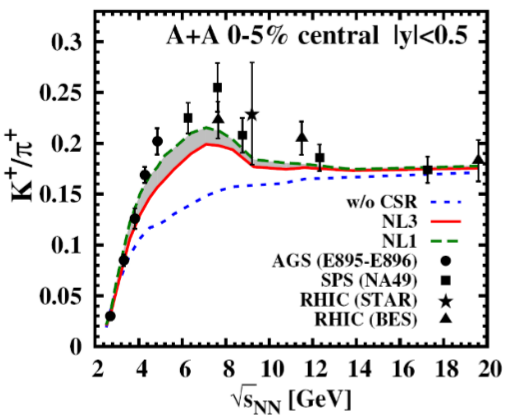

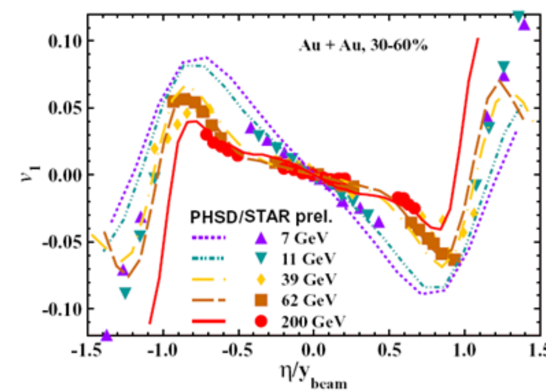

PHSD: P. Moreau

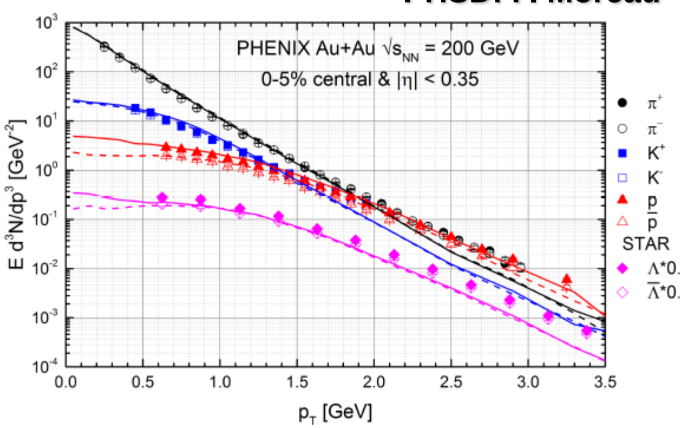

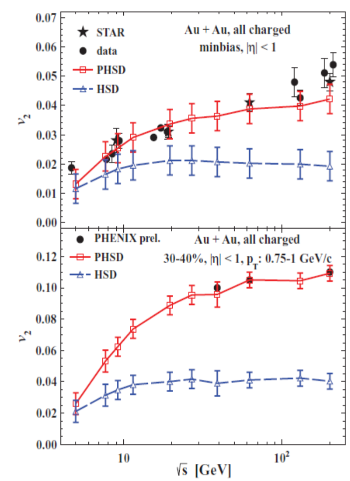

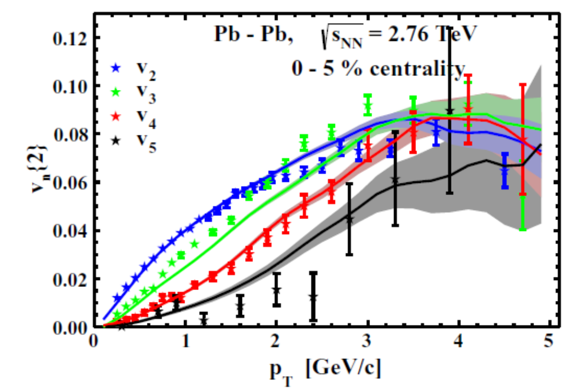

V. Konchakovski et al.,
PRC 85 (2012) 011902; JPG42 (2015) 055106

❑ **PHSD** provides a **good description of ‚bulk' observables** (y-, p_T-distributions, flow coefficients v_n, …) from SIS to LHC energies

Dynamics of heavy quarks – open charm and beauty (D/Dbar, B/Bbar) – in heavy-ion collisions

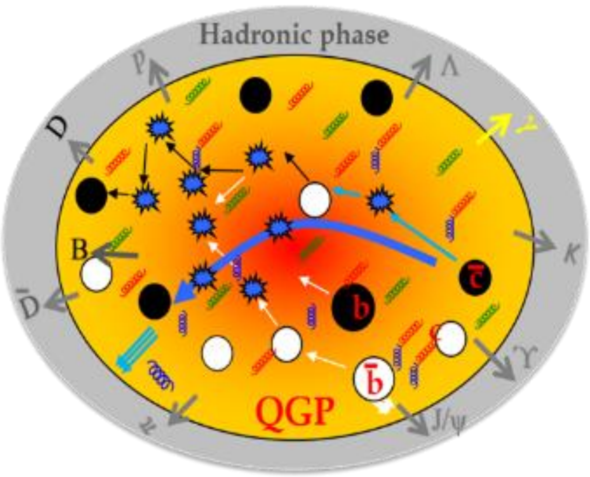

Charm dynamics in PHSD

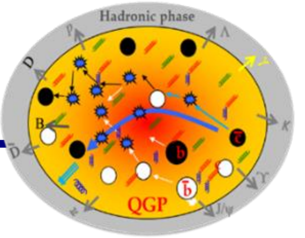

Dynamics of heavy quarks in A+A :

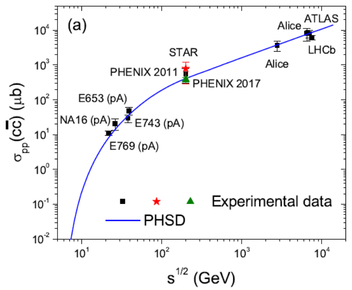

1. **Production** of heavy (charm and bottom) quarks in initial binary collisions + shadowing and Cronin effects

2. **Interactions in the non-perturbative QGP – according to the DQPM**: elastic scattering with off-shell massive partons Q+q→Q+q
   ➔ collisional energy loss

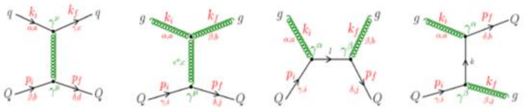

3. **Hadronization**: c/cbar quarks →D(D*)-mesons:

   Dynamical hadronization scenario for heavy quarks :
   coalescence with <r>=0.9 fm & fragmentation
   $0.4 < \varepsilon < 0.75$ GeV/fm³ $\varepsilon < 0.4$ GeV/fm³

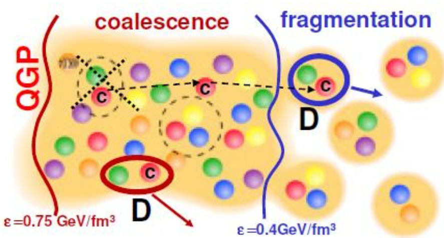

4. **Hadronic interactions**: D+baryons; D+mesons based on G-matrix and effective chiral Lagrangian approach with heavy-quark spin symmetry (>200 channels)
   (Juan Torres-Rincon, Laura Tolos)

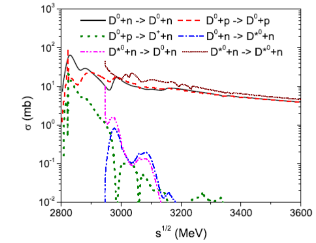

* PHSD references on charm dynamics:
Taesoo Song et al., PRC 92 (2015) 014910, PRC 93 (2016) 034906, PRC 96 (2017) 014905
PRC 97 (2018) 064907; PRC 101 (2020) 044901; PRC 101 (2020) 044903

Charm production in NN collisions

- A+A: charm production in initial NN binary collisions: probability $P = \dfrac{\sigma(c\bar{c})}{\sigma_{NN}^{inel}}$

The total cross section for charm production in p+p collisions $\sigma(c\bar{c})$

Momentum distribution of heavy quarks:
use ‚tuned' PYTHIA event generator to reproduce FONLL (fixed-order next-to-leading log) results

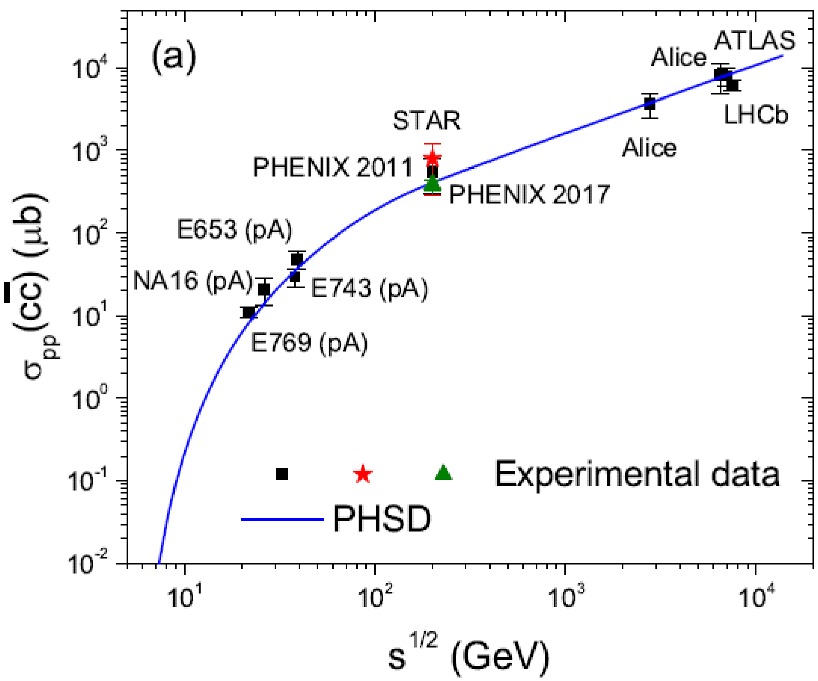

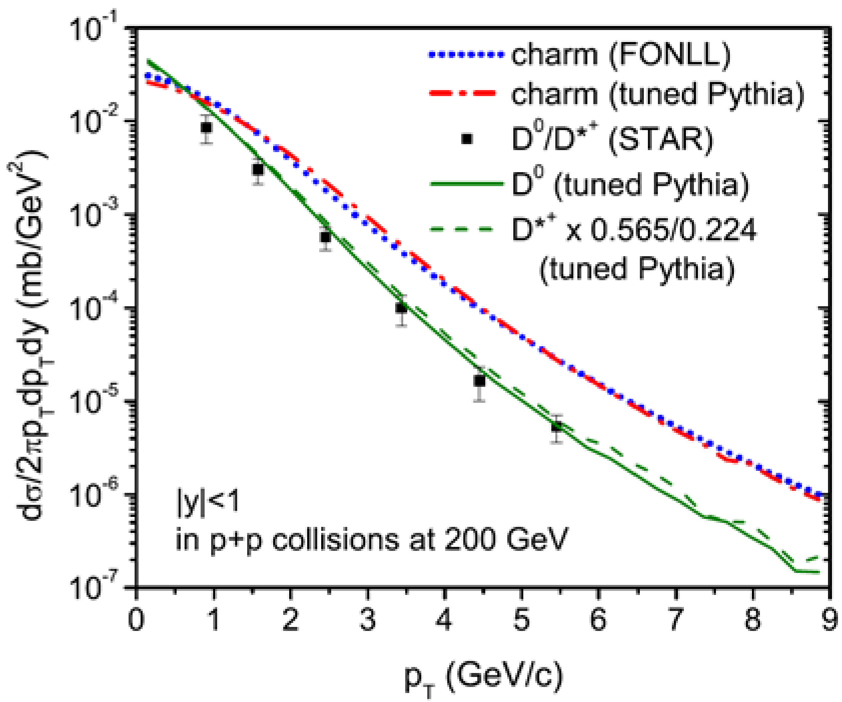

T. Song, W.Cassing, P.Moreau and E.Bratkovskaya, PRC 97 (2018) 064907

T. Song et al., PRC 92 (2015) 014910, PRC 93 (2016) 034906, PRC 96 (2017) 014905

Heavy quark scattering in the QGP (DQPM)

- Elastic scattering with **off-shell massive partons Q+q(g)→Q+q(g)**

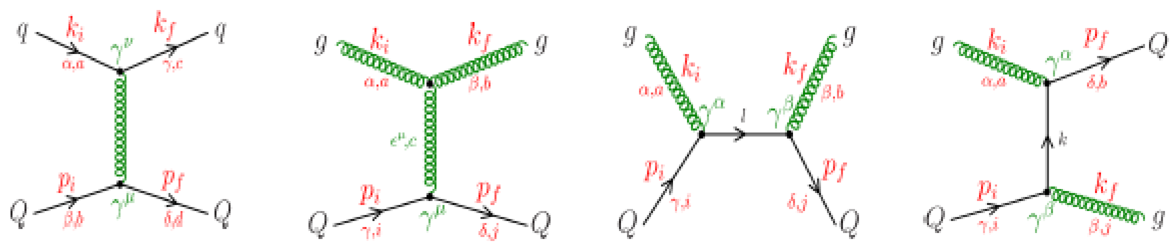

Non-perturbative QGP!

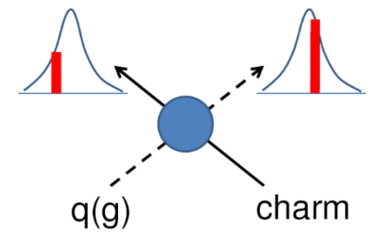

- Elastic cross section uc→uc

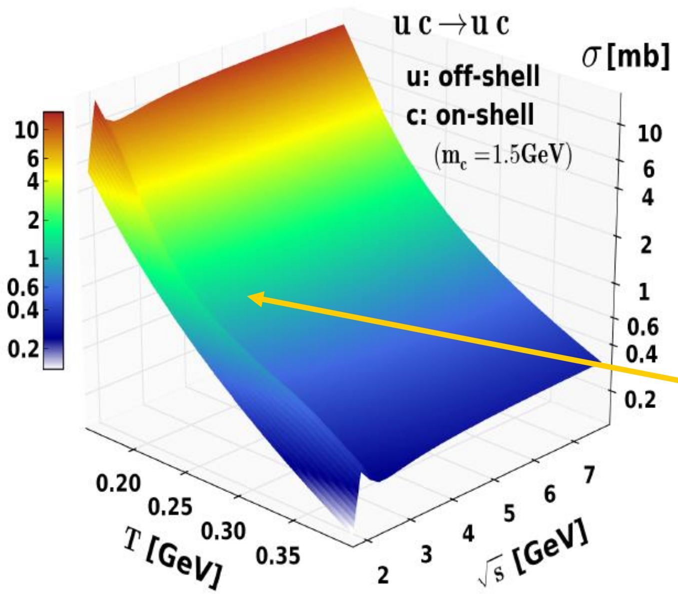

- Distributions of Q+q, Q+g collisions vs $s^{1/2}$ in Au+Au, 10% central

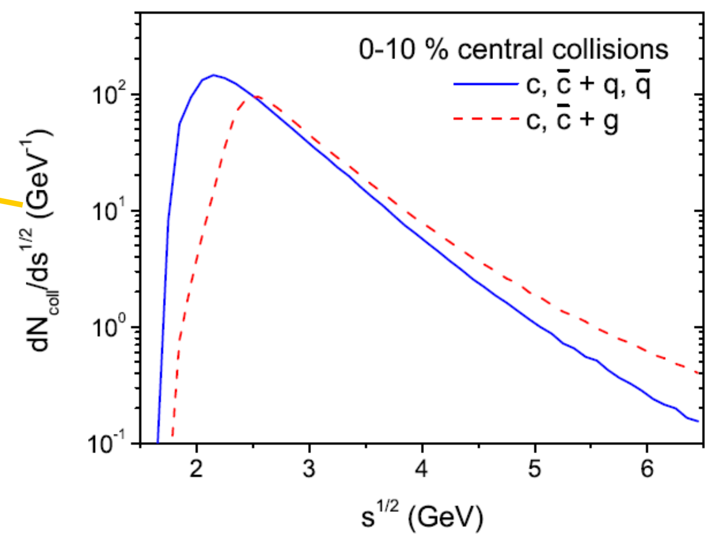

H. Berrehrah et al, PRC 89 (2014) 054901;
PRC 90 (2014) 051901; PRC90 (2014) 064906

Heavy quark scattering in the QGP

- **Differential elastic cross section for cq→cq, bq→bq for $s^{1/2}=s_0^{1/2}$ +2GeV at 1.5T_C**

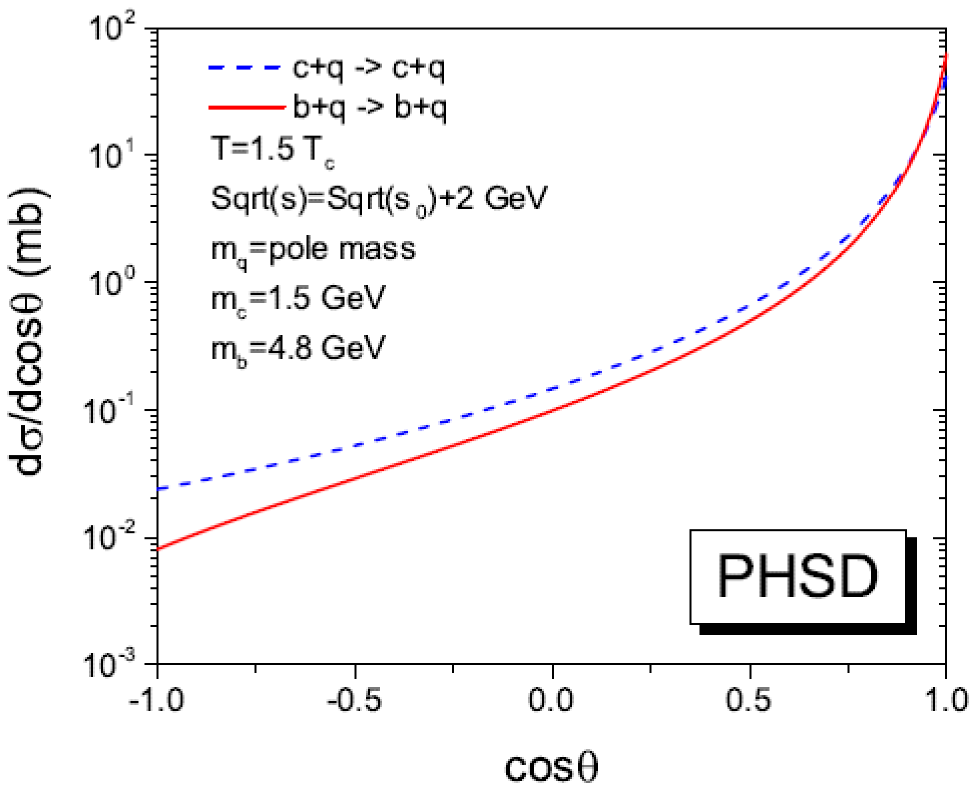

- **DQPM - anisotropic angular distribution**

Note: pQCD - strongly forward peaked
➔ Differences between DQPM and pQCD : less forward peaked angular distribution leads to more efficient momentum transfer

➔ Smaller number (compared to pQCD) of elastic scatterings with massive partons leads to a larger energy loss

! Note: radiative energy loss is NOT included yet in PHSD,
it is expected to be small (at low p_T) due to the large gluon mass in the DQPM

H. Berrehrah et al, PRC 89 (2014) 054901; PRC 90 (2014) 051901; PRC90 (2014) 064906

Charm spatial diffusion coefficient D_s

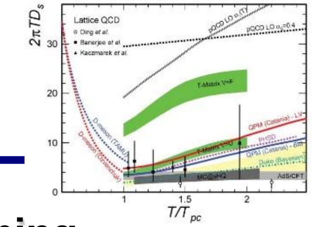

- **D_s for heavy quarks as a function of T for $\mu_q=0$ and finite μ_q assuming adiabatic trajectories (constant entropy per net baryon s/n_B) for the expansion**

$$D_s = lim(\vec{p} \to 0)\frac{T}{M\eta_D}$$ where η_D = A/p ; A(p,T) = drag coefficient

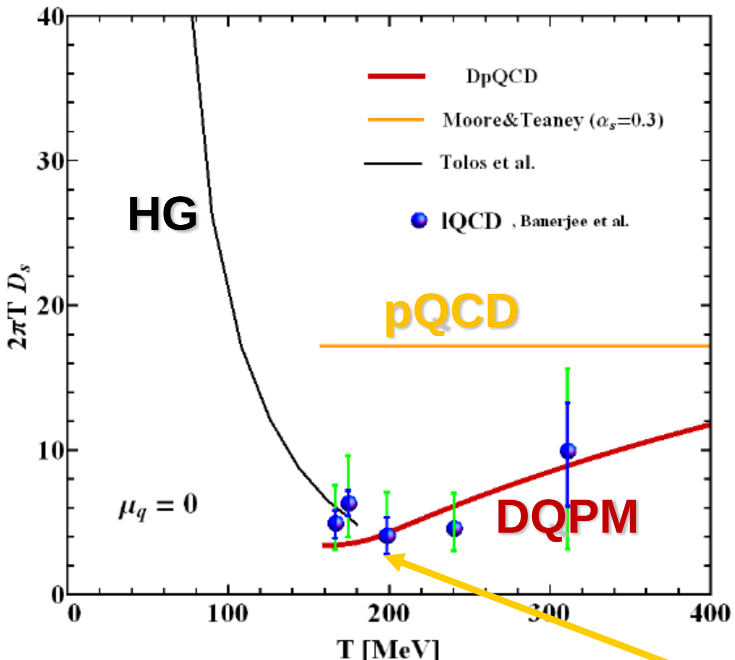

$\Rightarrow$ $\mu_q \neq 0$

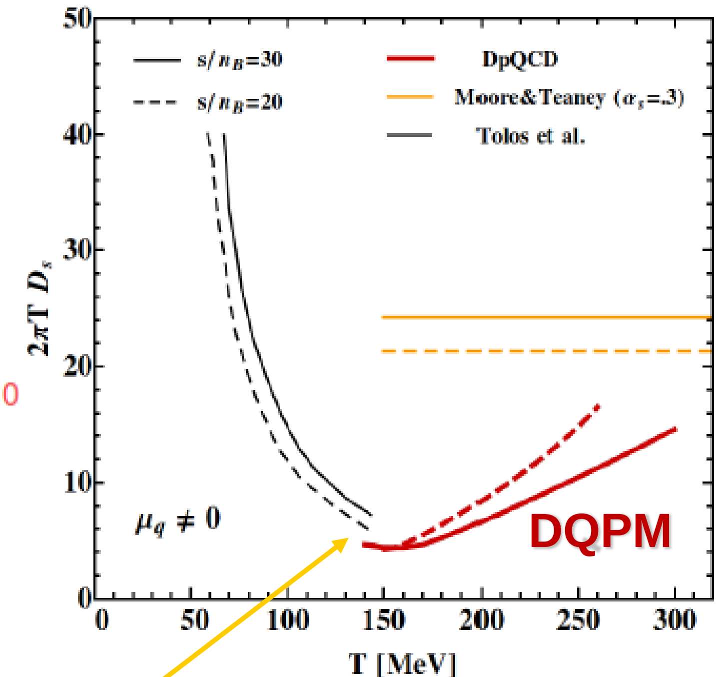

❑ **T < T_c : hadronic D_s**

L. Tolos , J. M. Torres-Rincon, PRD 88 (2013) 074019
V. Ozvenchuk et al., PRC90 (2014) 054909

➔ Continuous transition at T_C!

H. Berrehrah et al, PRC 90 (2014) 051901, arXiv:1406.5322

Hadronization of heavy quarks in A+A

- PHSD: if the local energy density $\varepsilon \rightarrow \varepsilon_C$ ➔ hadronization of heavy quarks to hadrons

T. Song et al., PRC 93 (2016) 034906

Dynamical hadronization scenario for heavy quarks :

coalescence with <r>=0.9 fm & fragmentation
0.4< ε < 0.75 GeV/fm³ ε < 0.4 GeV/fm³

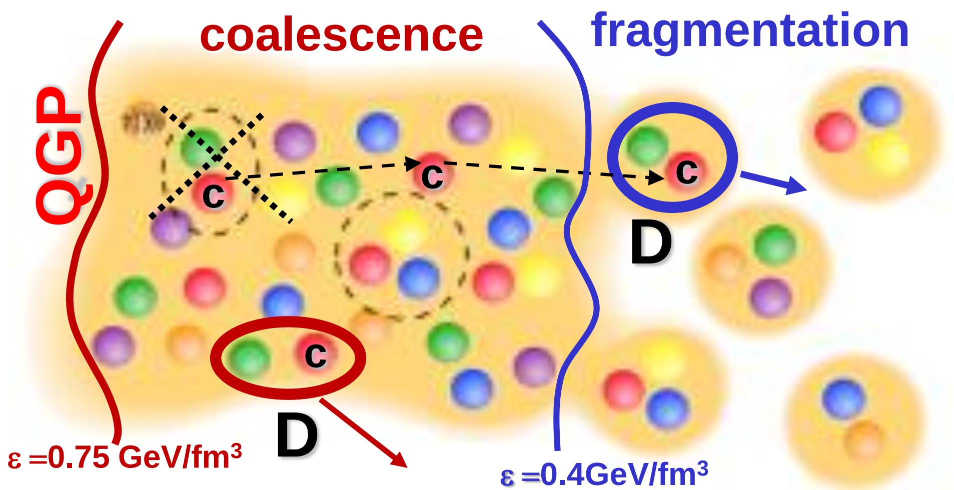

Coalescence probability in Au+Au at LHC

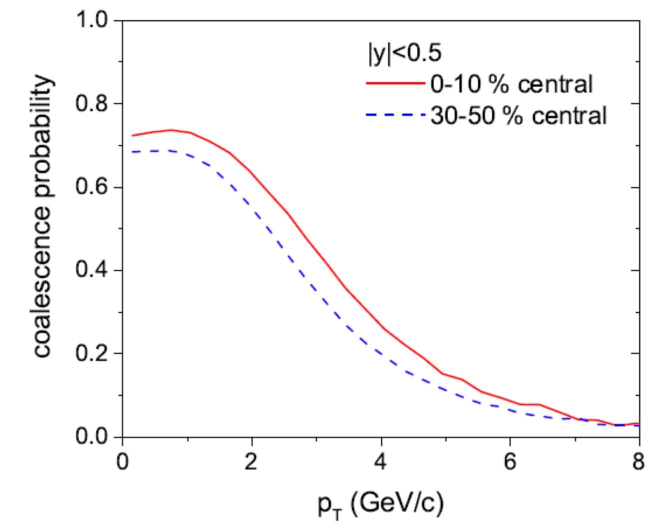

Coalescence probability for $c+\bar{q} \rightarrow D$

$$f(\boldsymbol{\rho}, \mathbf{k}_\rho) = \frac{8 g_M}{6^2} \exp\left[-\frac{\boldsymbol{\rho}^2}{\delta^2} - \mathbf{k}_\rho^2 \delta^2\right]$$

Width δ ← from root-mean-square radius of meson <r>:

where $\boldsymbol{\rho} = \frac{1}{\sqrt{2}}(\mathbf{r}_1 - \mathbf{r}_2), \quad \mathbf{k}_\rho = \sqrt{2}\, \frac{m_2 \mathbf{k}_1 - m_1 \mathbf{k}_2}{m_1 + m_2}$

$$\langle r^2 \rangle = \frac{3}{2} \frac{m_1^2 + m_2^2}{(m_1 + m_2)^2} \delta^2$$

Degeneracy factor : g_M = 1 for D, = 3 for $D^* = D^*_0(2400)^0$, $D^*_1(2420)^0$, $D^*_2(2460)^{0\pm}$

D-meson scattering in the hadronic phase

1. D-meson scattering with mesons

L. M. Abreu, D. Cabrera, F. J. Llanes-Estrada, J. M. Torres-Rincon, Annals Phys. 326, 2737 (2011)

Model: effective chiral Lagrangian approach with heavy-quark spin symmetry

Interaction of $D=(D^0,D^+,D^+_s)$ and $D^*=(D^{*0},D^{*+},D^{*+}_s)$ with octet (π,K,Kbar,η)

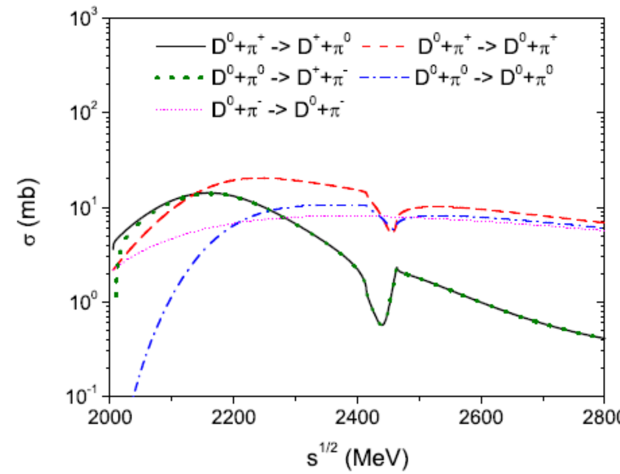

2. D-meson scattering with baryons

C. Garcia-Recio, J. Nieves, O. Romanets, L. L. Salcedo, L. Tolos, Phys. Rev. D 87, 074034 (2013)

Model: G-matrix approach: **interactions of $D=(D^0,D^+,D^+_s)$ and $D^*=(D^{*0},D^{*+},D^{*+}_s)$ with nucleon octet $J^P=1/2^+$ and Delta decuplet $J^P=3/2^+$**

Unitarized scattering amplitude ➔ solution of coupled-channel Bethe-Salpeter equations:

$$T = T + VGT$$

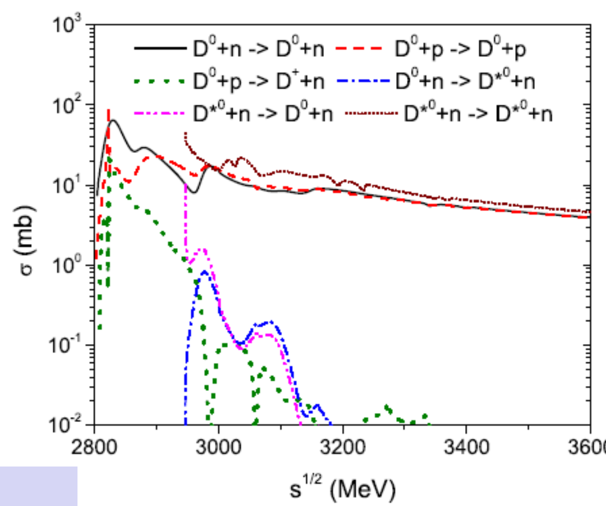

➔ Strong isospin dependence and complicated structure (due to the resonance coupling) of D+m, D+B cross sections!

B-meson scattering in the hadron gas

L. Tolos and J. M. Torres-Rincon, Phys. Rev. D 88, 074019 (2013)
J. M. Torres-Rincon, L. Tolos and O. Romanets, Phys. Rev. D 89, 074042 (2014)

1. B-meson scattering with mesons

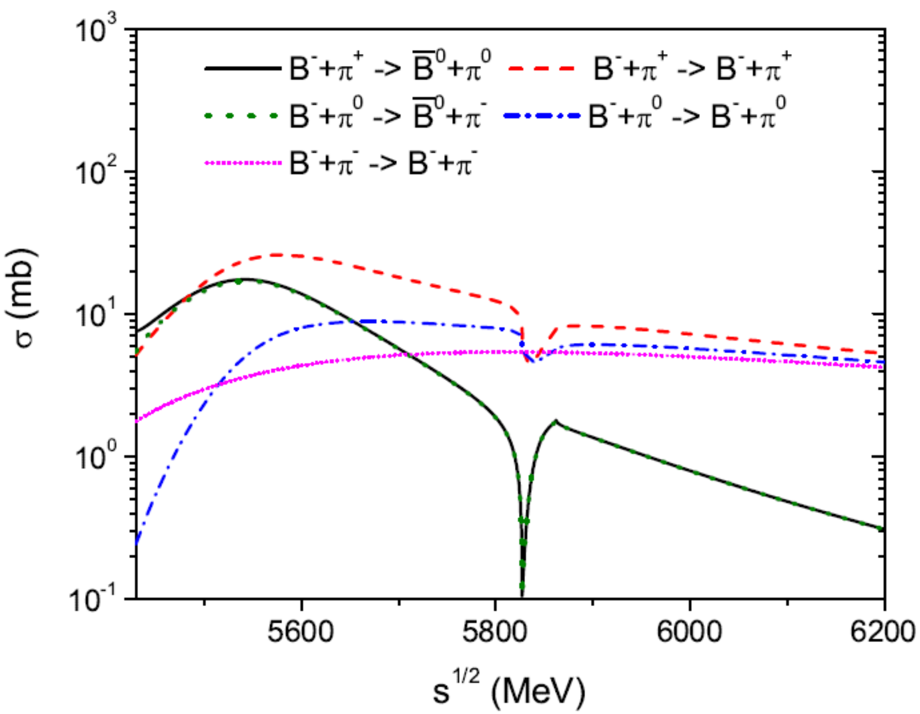

2. B-meson scattering with baryons

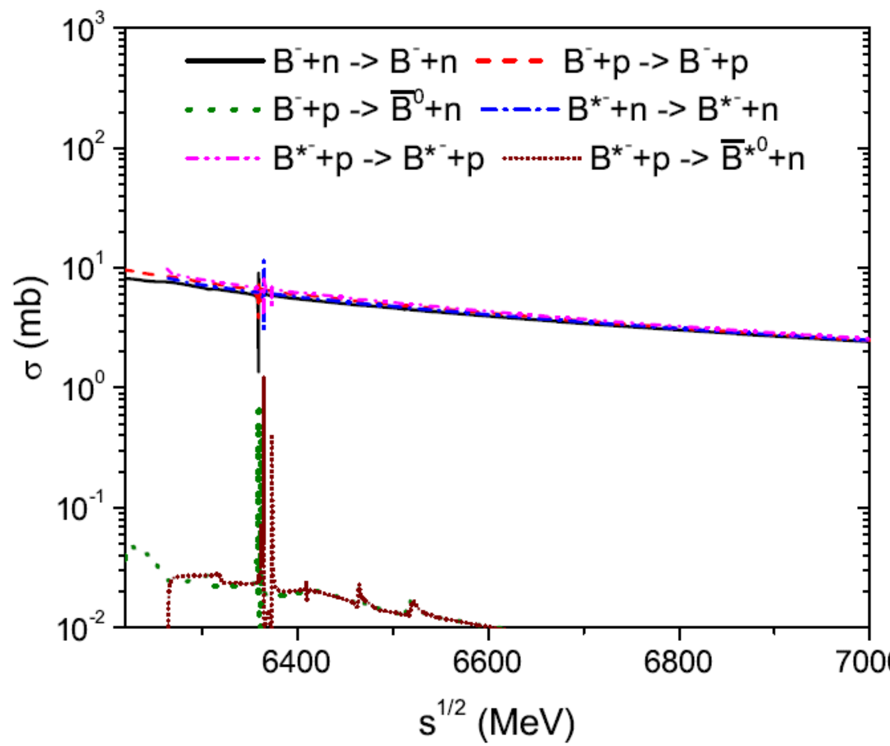

- **>200 hadronic channels** ➔ **implemented in the PHSD**

R_{AA} at RHIC - coalescence vs fragmentation

Influence of hadronization scenarios: coalescence vs fragmentation

! Model study: without any rescattering (partonic and hadronic)

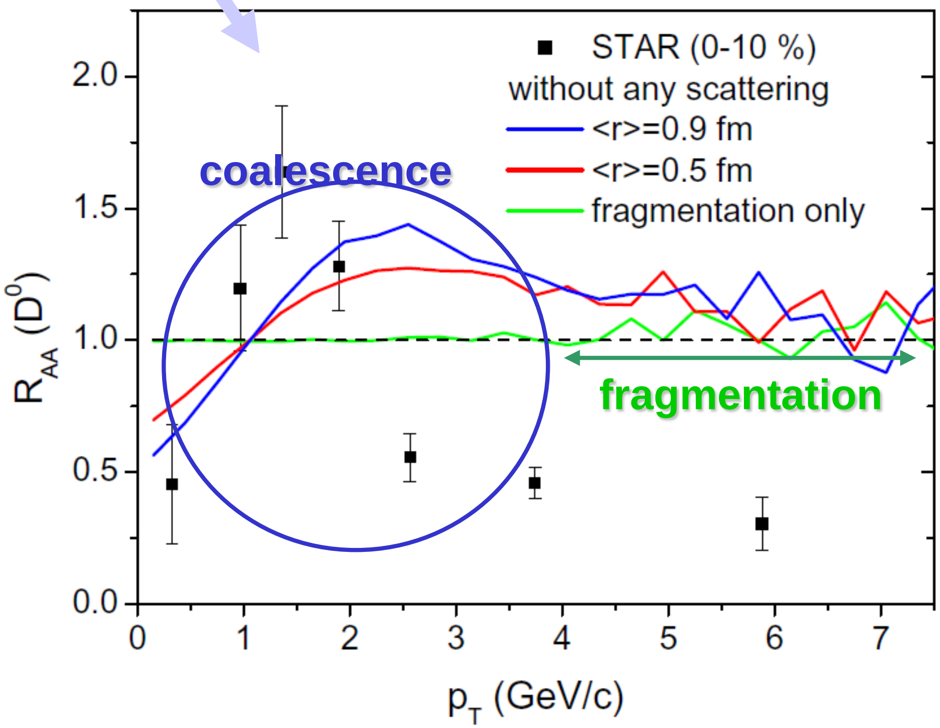

$$R_{AA}(p_T) \equiv \frac{dN_D^{\mathrm{Au+Au}}/dp_T}{N_{\mathrm{binary}}^{\mathrm{Au+Au}} \times dN_D^{\mathrm{p+p}}/dp_T}$$

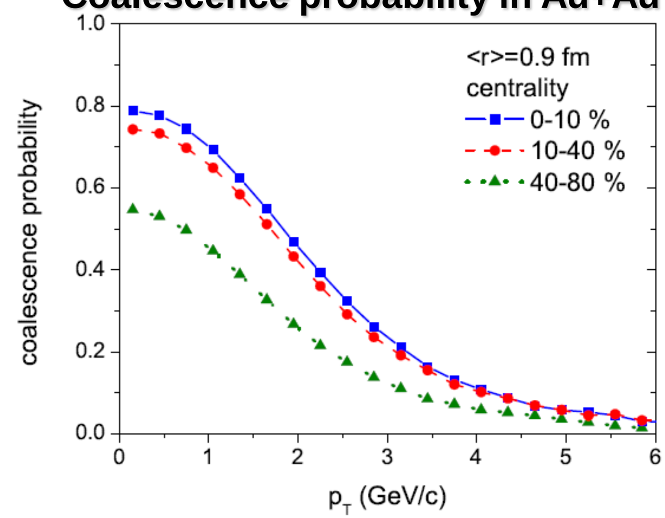

- **Expect: no scattering: R_{AA}=1**
- **Hadronization by fragmentation only (as in pp) ➔ R_{AA}=1**
- **Coalescence (not in pp!) shifts R_{AA} to larger p_T ➔ ‚nuclear matter‘ effect**
- **The hight of the R_{AA} peak depends on the balance: coalescence vs. fragmentation**

R_{AA} at RHIC: hadronic rescattering

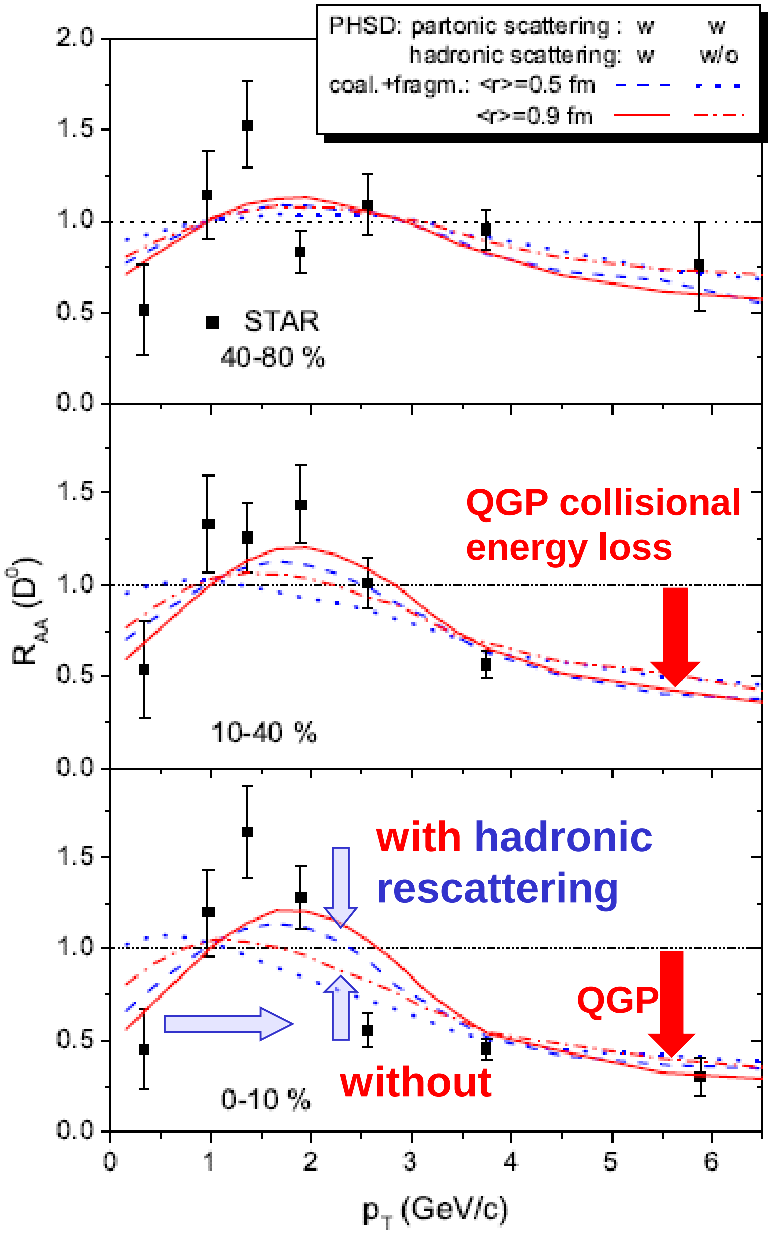

Influence of hadronic rescattering:

Central Au+Au at $s^{1/2}$ =200 GeV :

N(D,D*) ~30

N(D,D*+m) ~56 collisions

N(D,D*+B,Bbar) ~10 collisions

➔ each D,D* makes ~ 2 scatterings with hadrons

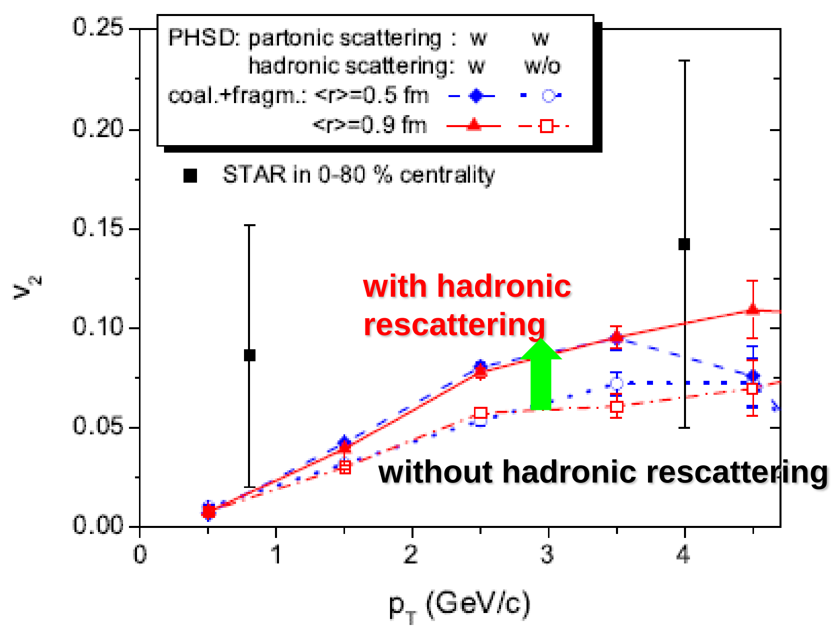

- **Hadronic rescattering moves R_{AA} peak to higher p_T !**
- **substantially increases v_2 at larger p_T**

T. Song et al., PRC 92 (2015) 014910

Cold nuclear matter effect: shadowing +Cronin

Shadowing effect: charm production is N*N* in HIC dominated by **gluon fusion**

$$\sigma_{c\bar{c}}^{N^*N^*}(s) = \langle R_g^{Pb}(x_1,Q) R_g^{Pb}(x_2,Q)\rangle \; \sigma_{c\bar{c}}^{NN}(s)$$

$R_i^A(x_1,Q)$, $R_i^A(x_2,Q)$ for *i=j=gluon* are obtained from the **EPS09 model**

K. J. Eskola, H. Paukkunen and C. A. Salgado, JHEP 0904, 065 (2009)

The modifications of the charm transverse momentum in N*N* vs NN due to the shadowing and Cronin effects in d+A and Au+Au @ 200 GeV

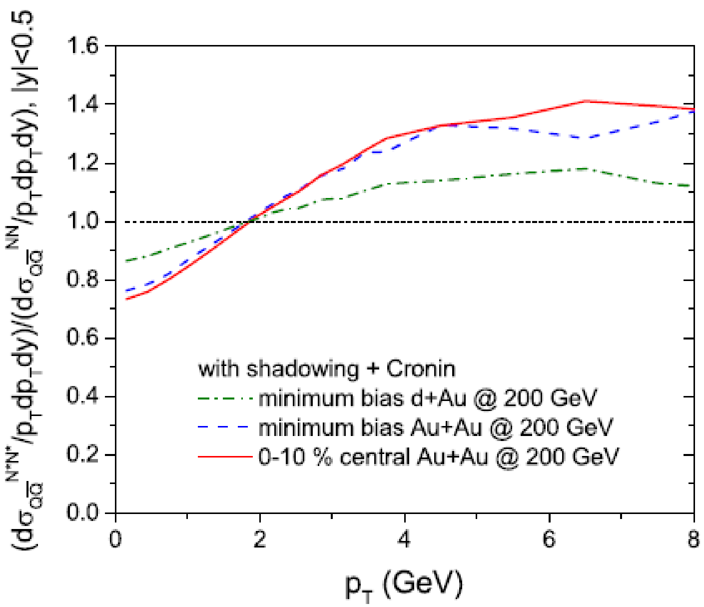

- **Shadowing effect** increases R_{AA} for low p_T
- **Cronin effect** increases R_{AA} for p_T >1 GeV

R_{AA} from single e^- (μ) in d+Au @ 200 GeV

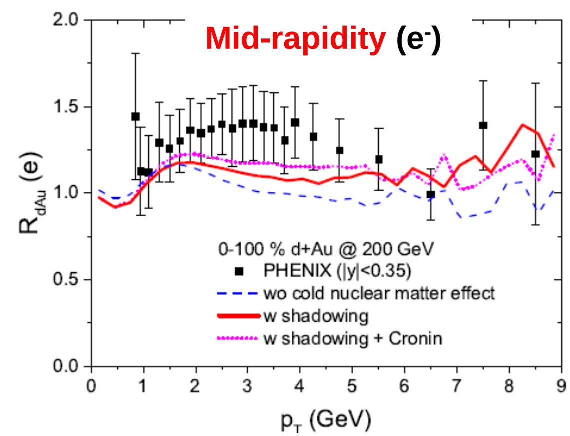

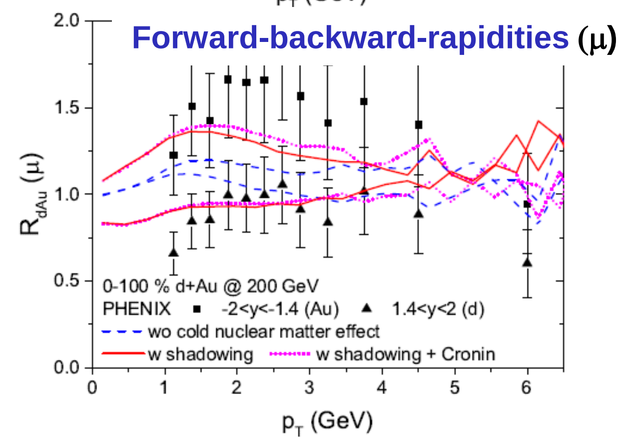

T. Song et al., PRC 96, 014905 (2017)

PHSD vs charm observables at RHIC

STAR

R_{AA} and v_2 vs p_T from D^0 -mesons in Au+Au @ 200 GeV →

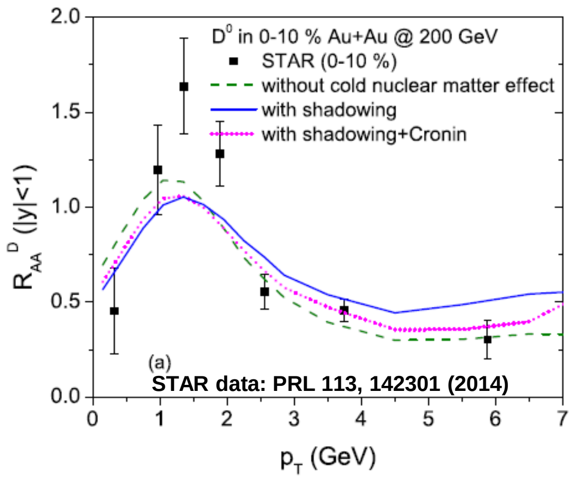

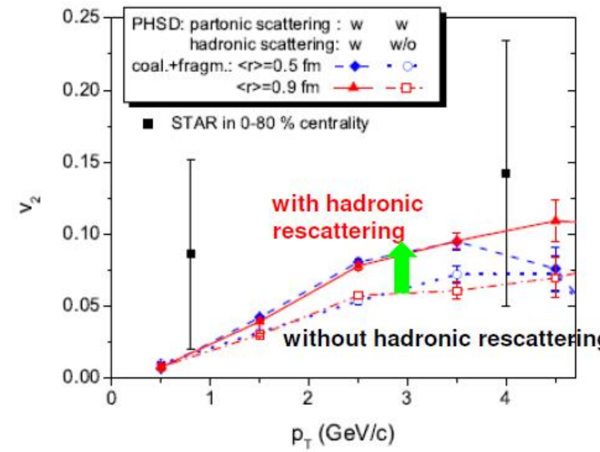

PHENIX

R_{AA} and v_2 vs p_T from single electrons in Au+Au @ 200 GeV →

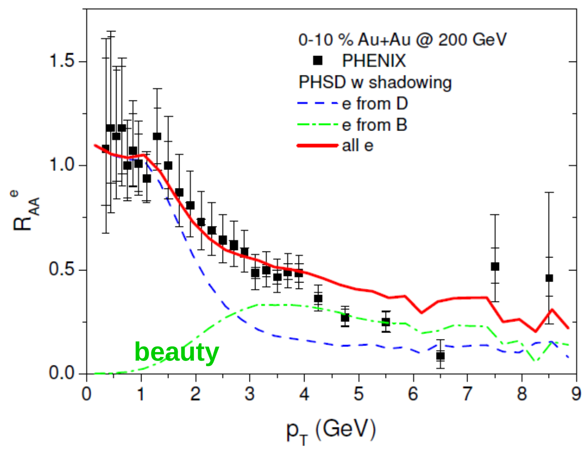

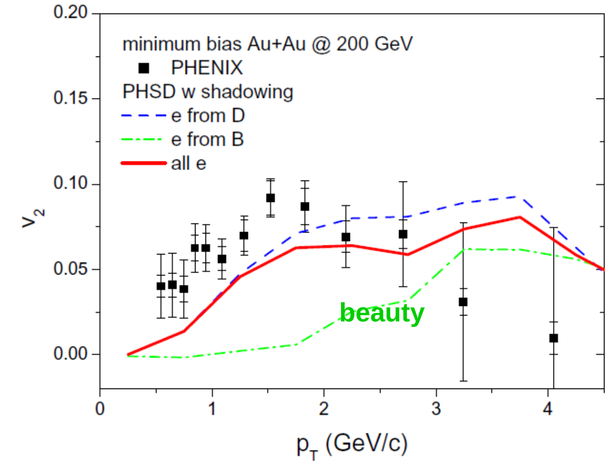

- The exp. data for the R_{AA} and v_2 are described in the PHSD by QGP collisional energy loss due to elastic scattering of charm quarks with massive quarks and gluons in the QGP
+ by the dynamical hadronization scenario „coalescence & fragmentation“
+ by strong hadronic interactions due to resonant elastic scattering of D,D* with mesons and baryons
- Feed back from beauty contribution becomes dominant for single electrons R_{AA} and v_2 at p_T >3 GeV

T. Song et al., PRC 92 (2015) 014910, PRC 93 (2016) 034906, PRC 96 (2017) 014905

Charm R_{AA} at LHC: PHSD vs ALICE

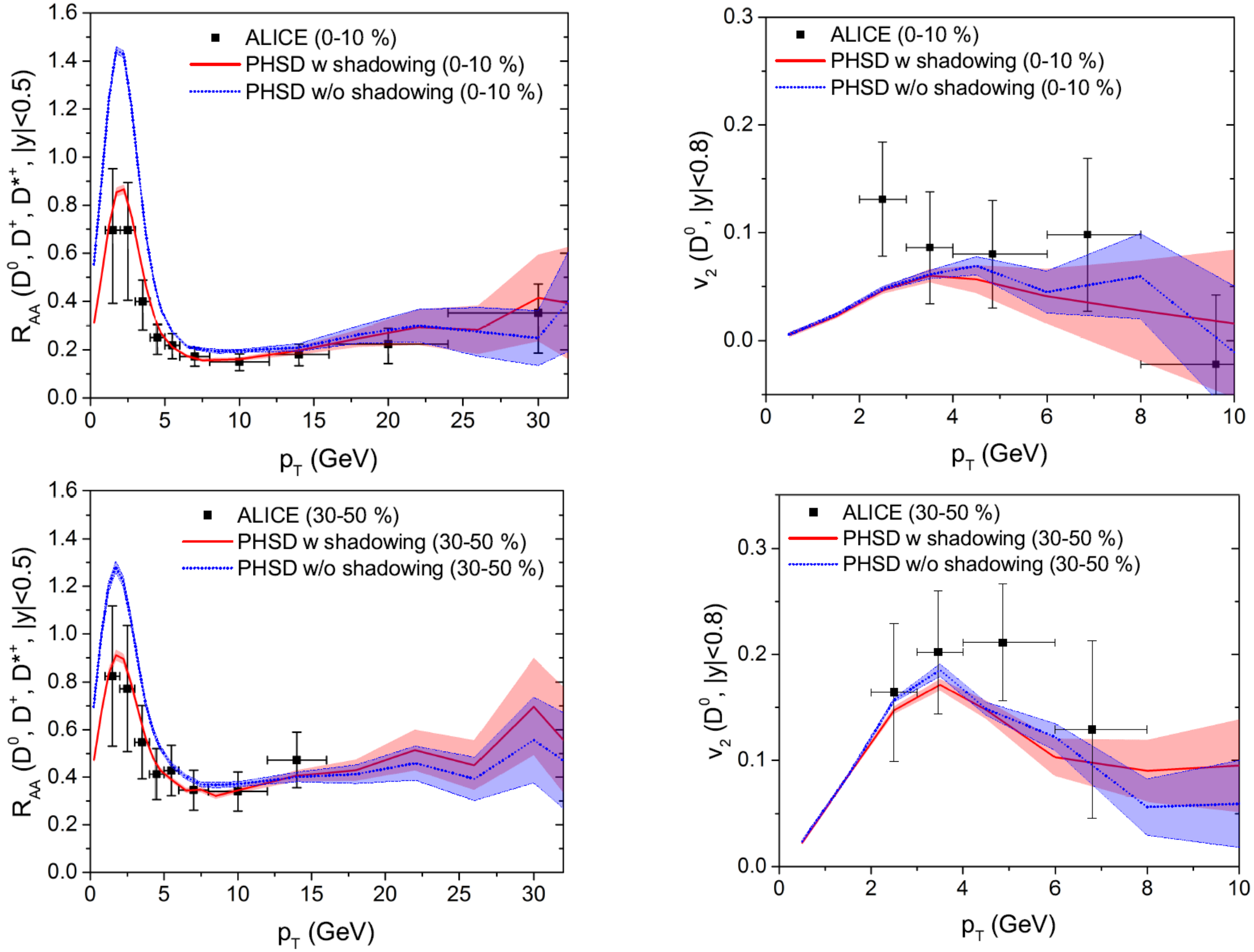

- in PHSD the energy loss of D-mesons at high p_T can be dominantly attributed to partonic scattering
- Shadowing effect suppresses the low p_T and slightly enhances the high p_T part of R_{AA}
- Hadronic rescattering moves R_{AA} peak to higher p_T; increases v_2

T. Song et al., PRC 93 (2016) 034906

PHSD vs charm observables at LHC (predictions)

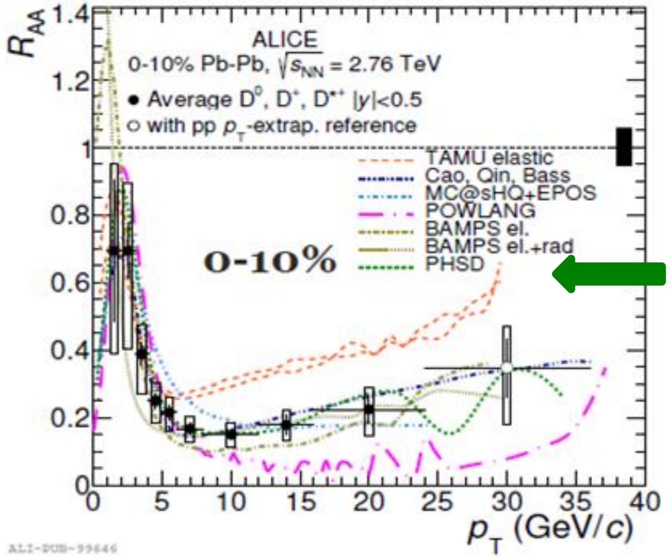

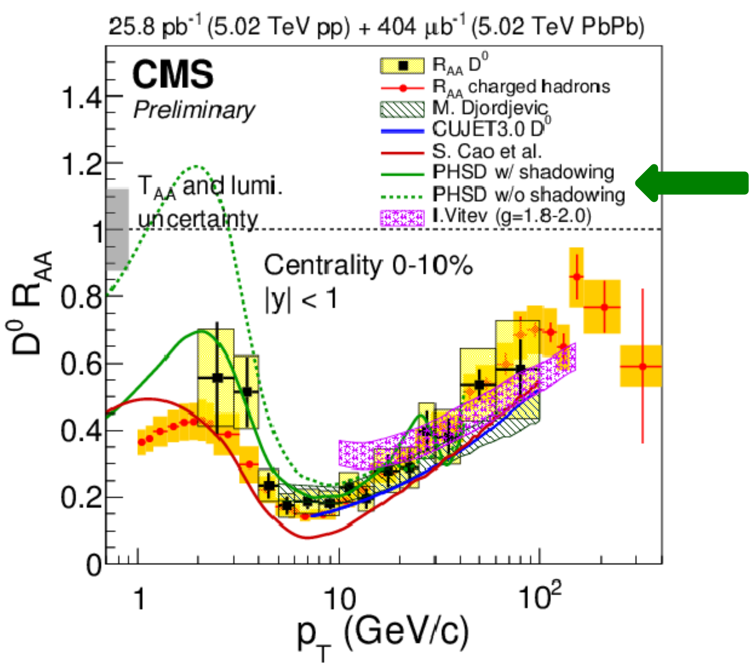

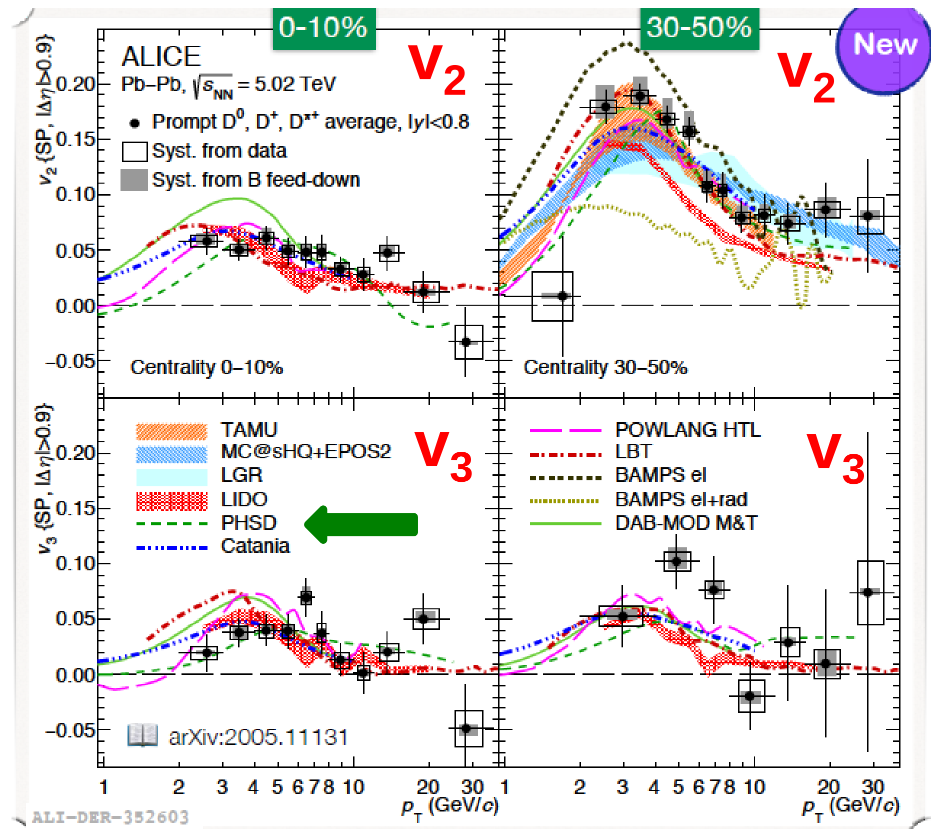

T. Song et al., PRC 92 (2015) 014910,
PRC 93 (2016) 034906, PRC 96 (2017) 014905

Energy gain/loss at RHIC

- **Transverse momentum gain or loss of charm quarks per unit time at mid-rapidity in 0-10 % central Au+Au collisions at $s^{1/2}$= 200 and 19 GeV**

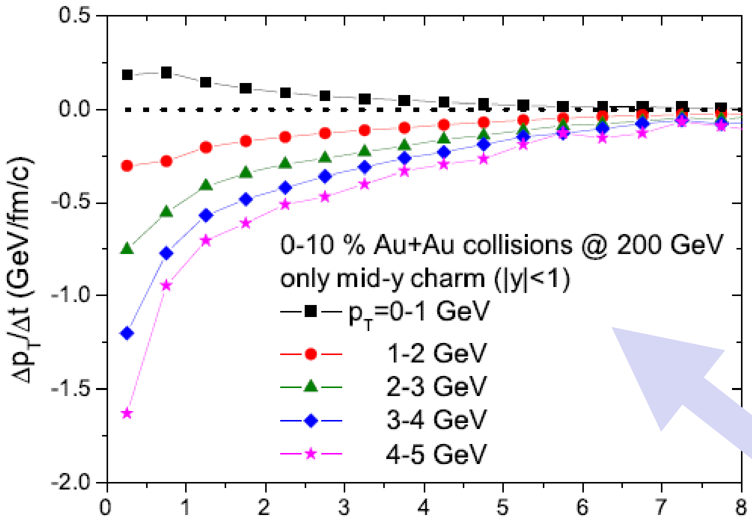

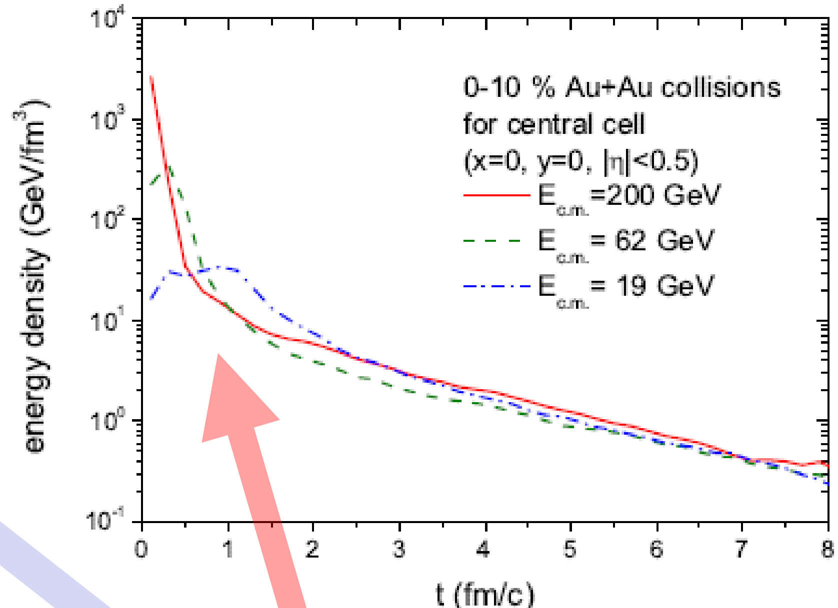

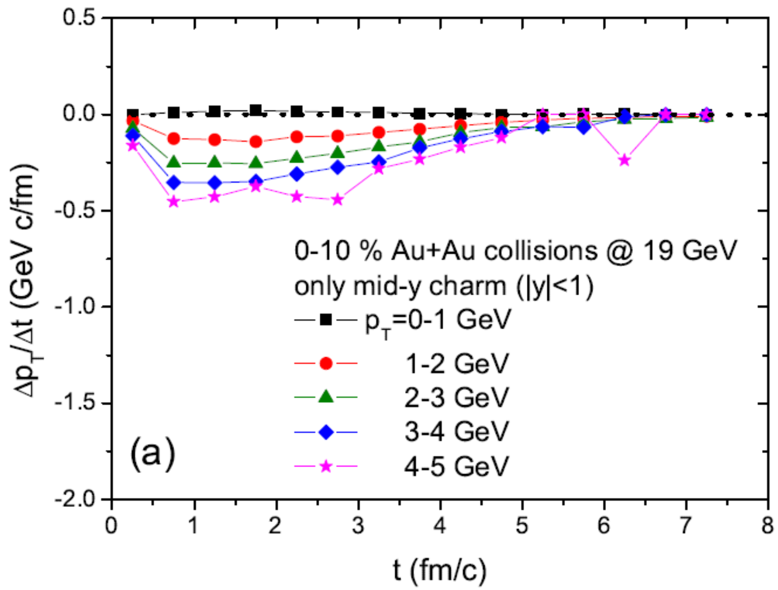

A considerable energy and transverse momentum loss happens in the initial stage of heavy-ion collisions during the QGP phase, because the energy density is extremely large

Thermalization of charm quarks in A+A ?

Model study

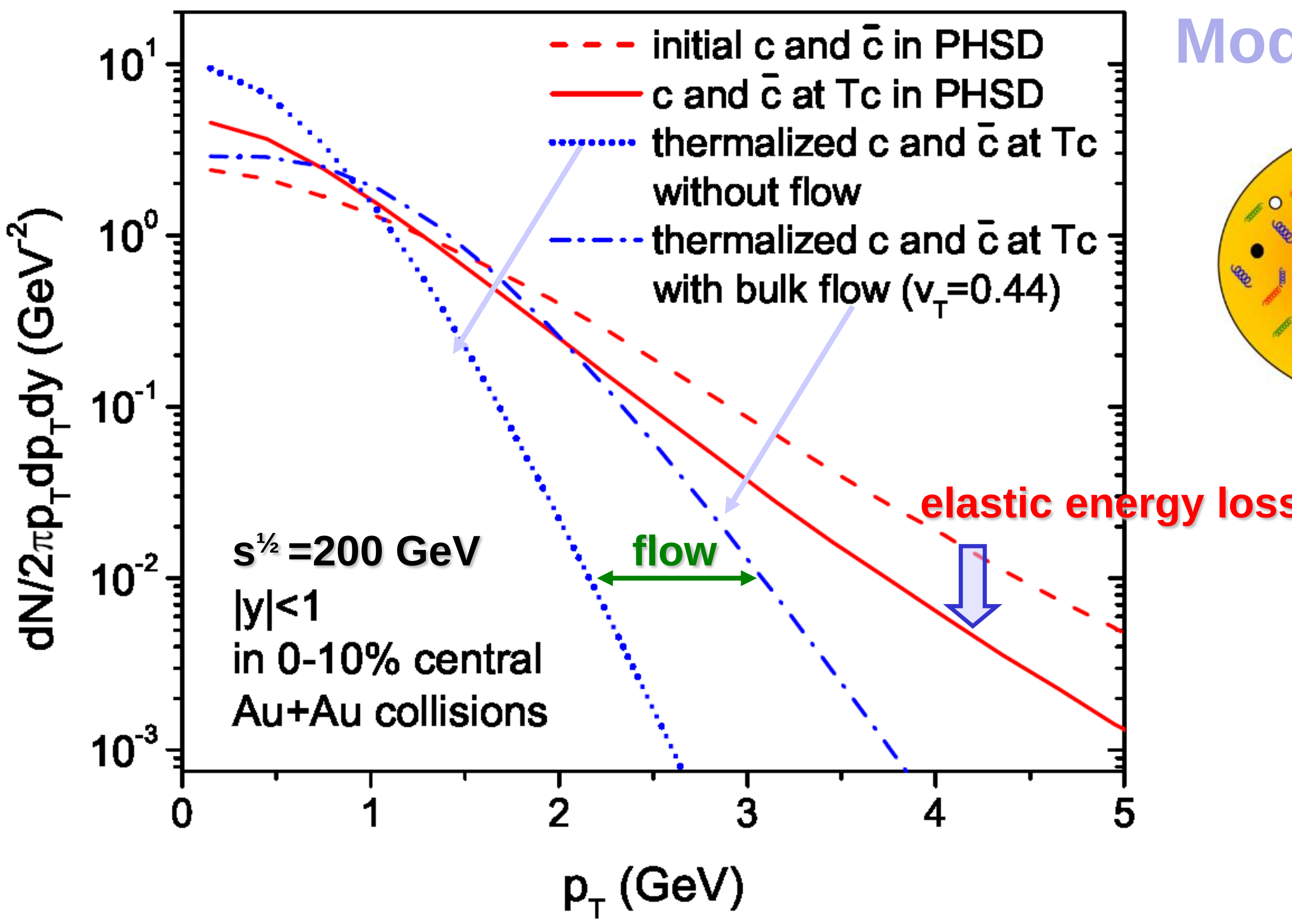

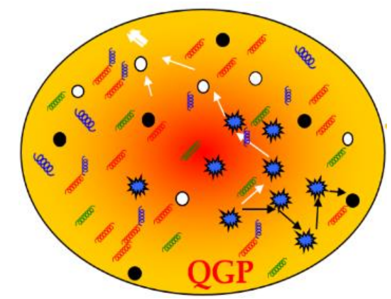

- Scattering of charm quarks with massive partons softens the p_T spectra
  ➔ elastic energy loss
- Charm quarks are close to thermal equilibrium at low p_T < 2 GeV/c

T. Song et al., PRC 92 (2015) 014910

Angular correlation between D-Dbar

Azimuthal angular distribution between the transverse momentum of D-Dbar at midrapidity ($|y| < 1$) before (dashed lines) and after the interactions with the medium (solid lines) in central Pb+Pb collisions at $s^{1/2} = 17.3$ and 200 GeV

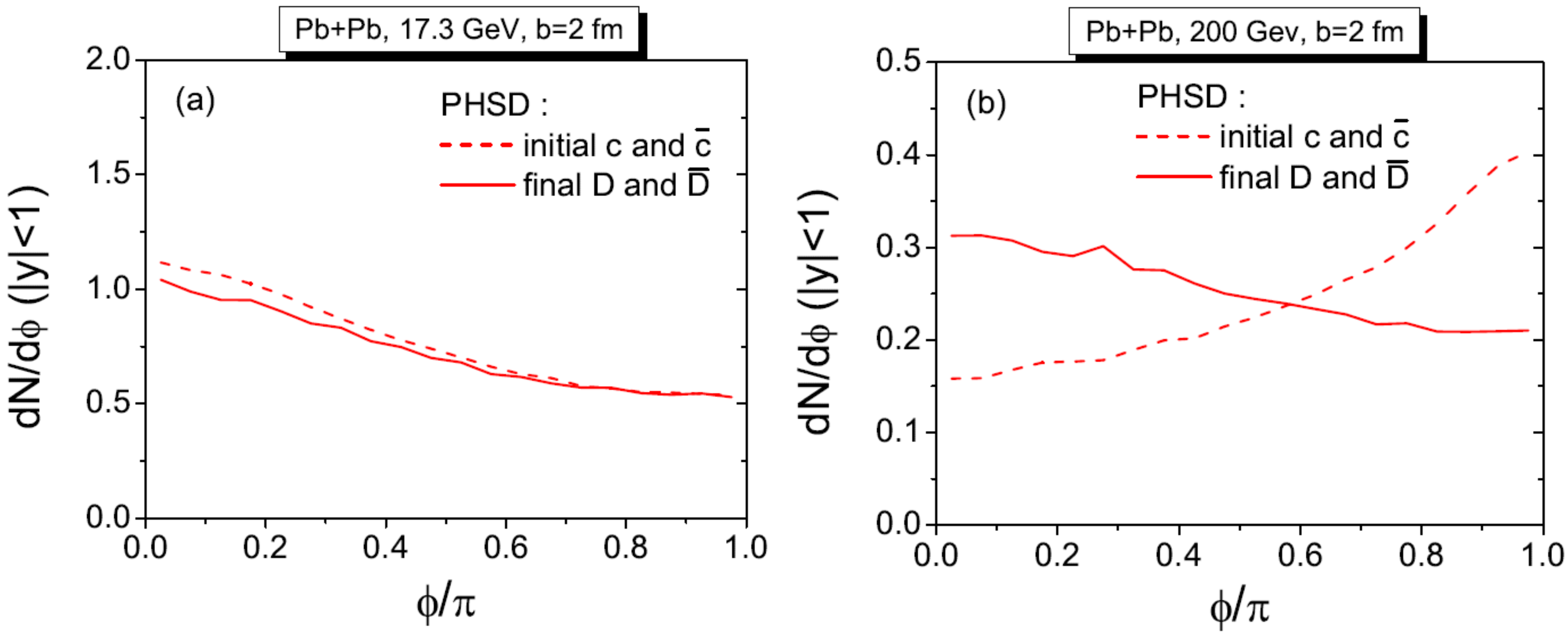

- Initial correlations - from PYTHIA : peaks around $\phi = 0$ for $\sqrt{s} = 17.3$ GeV, while around $\phi = \pi$ for $\sqrt{s} = 200$ GeV
- Final correlations: smeared at $\sqrt{s} = 200$ GeV due to the interaction of charm quarks in QGP

T. Song, W.Cassing, P.Moreau and E.Bratkovskaya, PRC 97 (2018) 064907

Summary

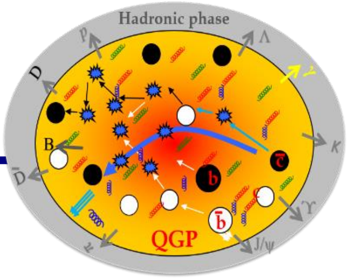

- **PHSD provides a microscopic description of non-equilibrium charm dynamics in the partonic and hadronic phases**

- **Partonic rescattering suppresses the high p_T part of R_{AA}, generates v_2**

- **Hadronic rescattering moves R_{AA} peak to higher p_T, increases v_2**

- **The structure of R_{AA} at low p_T is sensitive to the hadronization scenario, i.e. to the balance between coalescence and fragmentation**

- **Shadowing effects suppress R_{AA} at LHC at low transverse momenta, Cronin effect slightly increases R_{AA} above p_T >1 GeV**

- **The exp. data for the R_{AA} and v_2 at RHIC and LHC are described in the PHSD by QGP collisional energy loss due to the elastic scattering of charm quarks with massive quarks and gluons in the QGP phase**
  + by the dynamical hadronization scenario „coalescence & fragmentation“
  + by strong hadronic interactions due to resonant elastic scattering of D,D* with mesons and baryons

- **Feed back from beauty contribution for R_{AA}^e and v_2^e from single electrons for Au+Au at 200 GeV becomes dominant for p_T >3 GeV**

- **Initial azimuthal angular correlation of QQbar pairs is washed out during the evolution dominantly due to the transverse flow**